ELECTROCHEMICAL STUDIES ON CONDUCTING POLYMERS: COPOLYMERIZATION, ION TRANSPORT, RESTRUCTURING, OVEROXIDATION AND REACTIVATION

ZHIGANG QI

Electrochemical Studies on Conducting Polymers:

Copolymerization, Ion Transport, Restructuring,

Overoxidation and Reactivation

By

Zhigang Qi

A thesis submitted to the School of Graduate Studies in
partial fulfilment of the requirements for the degree of
Master of Science

Department of Chemistry
Memorial University of Newfoundland
St. John's, Newfoundland
Canada

November 1992

Canadä

To Li and Baby

ABSTRACT

The electrochemical copolymerization of 1-methyl-3-(pyrrol-1-ylmethyl)pyridinium ($MPMP^+$) with 3-methylthiophene (MeTh) has been accomplished from a wide compositional range of monomer solutions. An x-ray emission analysis method was developed to determine elemental composition and oxidation levels of such copolymers. A linear relationship was found to exist between the polymerization current density and the composition. The morphologies of the cationic copolymers were studied using scanning electron microscopy with the conclusion that surface roughness increases with increasing MeTh content and film thickness. Dual electrode and AC impedance measurements revealed that both the electronic and ionic conductivities of the copolymers increased with increasing MeTh content.

When poly($MeTh_x$-$MPMP^+$) was studied in aqueous $Fe(CN)_6^{3-/4-}$, it was found that the anodic to cathodic peak height ratios for $Fe(CN)_6^{3-/4-}$ were about 1:1 and 0.75:1 at fast and slow scan rates, respectively. This difference was concluded to arise from the competition between HPO_4^{2-} and $Fe(CN)_6^{3-/4-}$ during the redox process. HPO_4^{2-} is kinetically favoured, while $Fe(CN)_6^{3-/4-}$ is thermodynamically favoured as the charge compensating

counter ion in the copolymer. At fast scan rates, HPO_4^{2-} is the species that moves into and out of the copolymer to balance the excess charge during the redox process. At slow scan rates, $Fe(CN)_6^{3-/4-}$ transport balances the excess charge during the redox process. It was also found that $Fe(CN)_6^{4-}$ in the copolymer could not be replaced by HPO_4^{2-} even in aqueous 0.1 M K_2HPO_4, and that cations such as K^+ and Na^+ were not involved in the ion transport process.

Another finding was that the electrochemical response of a $Fe(CN)_6^{3-/4-}$ saturated copolymer decreased with time. Since x-ray emission analysis revealed that the amount of $Fe(CN)_6^{4-}$ in the film did not change during this decrease, it was realized that this decrease resulted from the formation of a strong association between $Fe(CN)_6^{4-}$ and the cationic sites in the copolymer. This association limits the mobility of $Fe(CN)_6^{4-}$ ions, which in turn leads to a slower charge transport rate between $Fe(CN)_6^{3-/4-}$ sites. The whole process has been termed restructuring of the copolymer film. The electrochemical activity of restructured copolymers could not be completely restored by ClO_4^- exchange and resaturated with $Fe(CN)_6^{3-/4-}$. Restructured films retarded the reentry of $Fe(CN)_6^{3-/4-}$ into the copolymer.

Two methods to reactivate poly(3-methylthiophene) films overoxidized in Cl⁻ solution have been discovered. The first is an electrochemical method. The overoxidized polymer was reactivated in Et_4NClO_4/acetonitrile when the potential exceeded 0.9 V. The other method is to oxidize the overoxidized polymer with 2,3-dichloro-5,6-dicyano-1,4-benzoquinone (DDQ). The overoxidation process is proposed to occur through a nucleophilic addition between oxidized poly-MeTh and Cl⁻. The reactivation process is believed to involve further oxidation of the overoxidized polymer with the elimination of protons. Oxidation of poly-MeTh in Br⁻ and I⁻ solutions is also discussed.

ACKNOWLEDGEMENTS

CONTENTS

LIST OF TABLES

LIST OF FIGURES

ix

LIST OF ABBREVIATIONS AND SYMBOLS USED

Symbol	Meaning	Unit
A	electrode area	cm^2
AC	alternating current	
bp	2,2'-bipyridine	
$(CH)_x$	polyacetylene	
C_p	concentration of a species in a polymer	mol/L
CV	cyclic voltammetry or cyclic voltammogram	
C_s	concentration of a species in a solution	mol/L
d	film thickness	μm
D	diffusion coefficient	cm^2/s
DDQ	2,3-dichloro-5,6-dicyano-1,4-benzoquinone	
D_p or D_{ct}	charge transport diffusion coefficient of a species in a polymer	cm^2/s
D_s	diffusion coefficient of a species in a solution	cm^2/s
E	potential	V
$E^{o'}$	apparent formal potential	V
$\Delta E_{Pt\text{-}Au}$	potential difference between the polymer coated electrode substrate and the overlying gold film in dual electrode voltammetry	V
ESR	electron spin resonance	
F	Faraday constant	96500 C/mol
FTIR	Fourier transform infrared	
HMH	simple representation of an aromatic monomer	
i or I	current	A
I_E	current at potential E in dual electrode voltammetry	A
i_{Lev}	Levich current	A

$i_{l,m}$	limiting current	A
INDO	intermediate neglect of differential overlap	
i_p or I_p	peak current	A
K	partition coefficient	
MeTh	3-methylthiophene	
MPMP$^+$	1-methyl-3-(pyrrol-1-ylmethyl)pyridinium ion	
MPMPBF$_4$	1-methyl-3-(pyrrol-1-ylmethyl)pyridinium tetrafluoroborate	
n	electrons per molecule involved in a redox process	
N	oxidation level	
P3-ETS	poly(thiophene ethanesulfonate)	
poly-MeTh	poly(3-methylthiophene)	
poly-MPMP$^+$	poly(1-methyl-3-(pyrrol-1-ylmethyl)pyridinium)	
poly(MeTh$_n$-MPMP$^+$)	poly{(3-methylthiophene)-co-[1-methyl-3-(pyrrol-1-ylmethyl)pyridinium]}	
pmp	3-(pyrrol-1-ylmethyl)pyridine	
Q_{cv}	voltammetric charge	C
Q_{pol}	polymer deposition charge	C
R	resistance	Ω
R_E	electronic resistance of an oxidized polymer	Ω
R_I	ionic resistance of an oxidized polymer	Ω
$R_{I,Red}$	ionic resistance of a reduced polymer	Ω
RMS	root mean square	
R_s	solution resistance	Ω
SSCE	saturated sodium chloride calomel electrode (0.24 V vs. standard hydrogen electrode)	
t	time	s
v	scan rate	V/s
ν	viscosity	cm^2/s
XPS	x-ray photoemission spectroscopy	
Z'	real impedance	Ω

Z"	imaginary impedance	Ω
σ	conductivity	$\Omega^{-1}cm^{-1}$
σ_E	electronic conductivity at potential E	$\Omega^{-1}cm^{-1}$
τ	experimental time scale	s

Chapter 1 INTRODUCTION TO CONDUCTING POLYMERS

1.1 HISTORY

In 1977, it was discovered that when the conjugated organic polymer, polyacetylene (Fig.1.1), was oxidized or reduced, its conductivity increased greatly with the resulting polymer having metallic properties [1]. This discovery transferred scientists' attention from the unsuccessful efforts of seeking analogous compounds to the inorganic conducting polymer, poly(sulfur nitride), $(SN)_x$ [2], to the synthesis of new organic conducting polymers. Two years later, conducting polypyrrole [3], poly(para-phenylene) [4] and poly(para-phenylene vinylene) [5] were successfully synthesized. The next year, poly(para-phenylene sulfide) [6, 7] and polythiophene [8] were reported. Since the 1977 discovery stimulated intense research in this area, it may represent the real beginning of the study of organic conducting polymers, although there were a few earlier reports of conducting polymers [9].
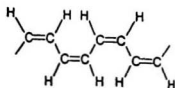
cis
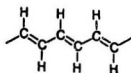
trans

Fig.1.1. Polyacetylene.

1.2 SYNTHETIC METHODS

1.2.1 Chemical Methods

Fig.1.2 summarizes the synthesis of conjugated polymers through chemical methods [10]. Both direct and indirect routes have been used. In the direct route A, the appropriate monomer is converted directly into a conjugated polymer. The conversion is usually via either an addition or a condensation process. The indirect route B consists of two steps. The first step is the synthesis of a precursor polymer by an addition or condensation polymerization procedure. This is followed by conversion of the precursor polymer into a conjugated polymer through one of a variety of different methods such as elimination, addition or isomerization.

1.2.2 Electrochemical Methods

A number of conducting polymers can be directly synthesized through electrochemical oxidation of the monomer under appropriate conditions [11-13]. Appropriate conditions involve proper selections of the solvent, supporting electrolyte, electrode material and potential. The oxidation can be carried out either galvanostatically (i.e., at constant current), potentiostatically (i.e., at constant potential), or under potential cycling.
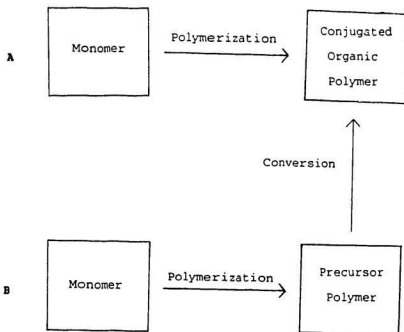
Fig.1.2. Chemical synthesis of conjugated polymers [10]: A--direct route; and B--indirect route.

Electrochemical polymerization reactions generally proceed stoichiometrically. Equation 1.1 shows the oxidative polymerization reaction for pyrrole, where HMH represents a pyrrole monomer with hydrogen atoms on its active 2 and 5 carbon positions (α positions). Reaction 1.1 can be viewed as occurring in two steps as indicated by equations 1.2 and

$$(n+2)HMH \rightarrow HM(M)_nMH^{(nx)+} + (2n+2)H^+ + (2n+2+nx)e^- \qquad (1.1)$$

$$(n+2)HMH \rightarrow HM(M)_nMH + (2n+2)H^+ + (2n+2)e^- \qquad (1.2)$$

$$HM(M)_nMH \rightleftharpoons HM(M)_nMH^{(nx)+} + (nx)e^- \qquad (1.3)$$
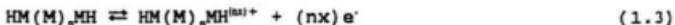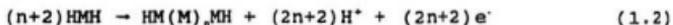
1.3 [13]. Each monomer molecule consumes about 2.1 to 2.5 electrons during its polymerization, while only two electrons are required for the formation of polypyrrole chains (Eq.1.2). The extra charge results from the oxidation of the polymer film which accompanies its formation (Eq.1.3). The positive charge on the polymer chains is compensated by anions which come from the supporting electrolyte. It has been observed that during the polymerization reaction, the solution becomes increasingly acidic [14]. This is consistent with the elimination of protons during electrochemical polymerization (Eq.1.1).

The advantages of electrochemical polymerization over chemical polymerization are that the conducting polymer is generated as a film on the working electrode in one step, and the growth or thickness of the polymer film can be controlled easily. Also, the properties of the polymer film, such as conductivity and morphology, can be varied by appropriate selections of the solvent and supporting electrolyte [13], as well as current density (see section 3.2.5).

Cyclic voltammetry is a simple method for determining whether a monomer can be electrochemically polymerized to form a conducting polymer. For an oxidative polymerization, an oxidation peak due to oxidation of the monomer will be seen during the first anodic scan. If a conductive polymer is formed, a small reduction current may be observed during the cathodic scan. Repeated scans will show increasing anodic and cathodic currents due to oxidation and reduction of the polymer film. Also, an oxidation peak due to the monomer will still be observed. On the other hand, if a non-conductive film is formed, no cathodic current will be observed during cathodic scans, and the anodic current due to oxidation of the monomer will decrease during successive scans. This is because the thin layer of nonconductive film formed on the

working electrode during the first oxidation scans blocks current flow, and thus prevents further oxidation of the monomer.

1.3 ELECTROCHEMICAL POLYMERIZATION OF PYRROLES AND THIOPHENES

1.3.1 Polymerization Mechanism

The electrochemical polymerization mechanism for pyrroles or thiophenes is still debatable. Two mechanisms have been proposed. One assumes that polymerization proceeds via a coupling reaction between a radical cation and a neutral monomer [15]. The other proposes that coupling reactions occur between radical cation intermediates [16].

The second mechanism, shown in Fig.1.3, is generally accepted at present, and is supported by a recent fast double potential step chronoamperometry investigation [17]. The first step involves oxidation of the monomer to its radical cation. After this initial oxidation step, there is a coupling reaction between radical cations, which is followed by deprotonation to form a neutral dimer. The dimer is then oxidized to a dimeric radical cation which couples with another radical cation to form a trimer after deprotonation. These processes continue and lead to the formation of a
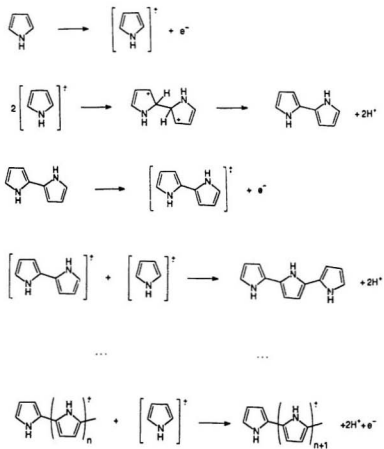
Fig.1.3. A proposed mechanism for the electrochemical polymerization of pyrrole [16].

conjugated polymer. As the oligomers produced in the polymerization become larger, they become easier to oxidize [18, 19], and their radical cations become less reactive [20]. However, polymerization is sustained because reactive monomeric radical cations, which react with the oligomeric radical cations, are continuously produced.

Chronoabsorptometric studies have revealed that polypyrrole films grow linearly with time t, and not $\sqrt{t}$ at a constant potential [16]. This finding was supposed to imply that the rate-limiting step during film growth is radical cation formation or coupling, and not the diffusion of monomer to the electrode surface [16, 21].

1.3.2 Linkage of Monomer Units

Since α,α'-blocked 2,5-dimethylthiophene and 2,5-dimethylpyrrole can not be polymerized electrochemically [11, 22], and oxidative degradation of chemically synthesized polypyrrole yielded primarily 2,5-disubstituted products [23], it has been realized that oxidative polymerization of pyrroles or thiophenes proceeds through coupling at the α-positions. Nuclear magnetic resonance studies have also suggested that polypyrrole is primarily α,α'-linked [24]. However, XPS (x-ray photoemission spectroscopy) studies showed that as many as

9

one out of three pyrrole rings was affected by structural disorder, part of which might be attributed to β-linkages [25]. Thus, when pyrroles or thiophenes are polymerized, although the monomer units are linked with each other mainly at the α-positions, a significant number of the units may be coupled through the β-positions. Coupling at the β-positions introduces defects in the ideal polymer chain arrangement. These defects reduce a polymer's conjugation length, and therefore its conductivity.

Taking advantage of the known correlation between reactivity and the unpaired electron density distribution of a radical cation [19], and utilizing pyrrole as an illustrative example, Waltman and coworkers have applied INDO (intermediate neglect of differential overlap) [26] molecular orbital calculations to explore the reactivities of the α and β positions of the monomer and oligomer radical cations [12, 20]. They found that the delocalized pyrrole radical cation has the highest unpaired electron density at its equivalent α-positions (Fig.1.4); accordingly, when two pyrrole radical cations dimerize, coupling can be expected to occur at the α-positions. However, the reactive sites in the oligomer radical cations become chemically inequivalent to those of the monomer radical cation. Thus, with increasing chain length,

the unpaired electron becomes increasingly delocalized so that the unpaired electron density difference between α- and β-positions becomes smaller. For example, in the trimer radical cation, the unpaired electron density at the 3,3"-positions is approximately equal to that at the 5,5"-positions (Fig.1.4). Therefore, these positions are about equally reactive without consideration of steric effects. Extension of this concept predicts that whereas initially the oxidative electrochemical polymerization of pyrrole might result in a rather regularly α-linked polymer, a more irregular connection pattern can be expected to result during later stages of the chain growth. The number of linkages involving the β-positions are predicted to increase with increasing chain length.

1.3.3 Solvent and Electrolyte

Since electrochemical polymerization proceeds via radical cation intermediates, the reaction is sensitive to the nucleophilicity of the surrounding species. Nucleophilic species may attack the radical cations and lead to the formation of soluble oligomers rather than a polymer film. Therefore, solvents and supporting electrolytes with low nucleophilicity are preferable [13]. The nucleophilicity of the commonly used solvents rises in the following order: SO_2 < CH_3NO_2 < CH_2Cl_2 < PC (propylene carbonate) < CH_3CN < H_2O [27].

pyrrole   2, 2'; 5', 2" - terpyrrole

(A)

(B)
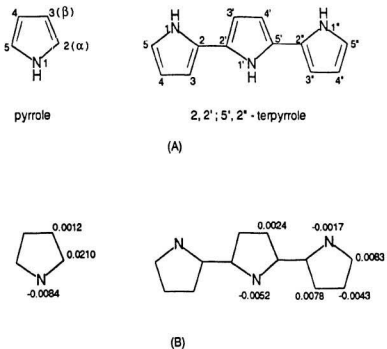
Fig.1.4. The numbering scheme (A) and unpaired electron distribution (B) of pyrrole and 2,2':5',2"-terpyrrole radical cations [20].

Among these solvents, acetonitrile is used most commonly. However, polypyrrole can be prepared in aqueous solutions [13] because the pyrrole radical cation is comparatively stable to H_2O.

With regards to the supporting electrolyte, its solubility and degree of dissociation must be considered in addition to its nucleophilicity. Most often tetraalkylammonium salts are used, because they are soluble and highly dissociated in aprotic solvents [13]. Lithium, sodium and potassium salts are seldom used, because lithium salts are generally aggregated, and sodium and potassium salts are poorly soluble in aprotic solvents. The most commonly used anions are ClO_4^-, BF_4^-, PF_6^-, AsF_6^-, $CF_3SO_3^-$ and $CH_3C_6H_4SO_3^-$ (p-toluenesulphonate). Highly nucleophilic anions, such as halides, hydroxide, alkoxide, and cyanide are seldom used [13].

1.3.4 Polymerization Efficiency

Electrochemical polymerization is usually affected by the electrode material, solvent, supporting electrolyte, purity of the monomer, and current density or potential employed. The polymerization efficiency is seldom 100% because of loss of soluble oligomers and side reactions [28]. After a radical

cation is formed, it can (1) polymerize to form a polymer film on the electrode surface; (2) diffuse away from the electrode to form some soluble species; or (3) react with the solvent, the anion of the supporting electrolyte, or an impurity (especially water) in the vicinity of the electrode surface. The polymerization efficiency is the fraction of radical cations which take part in the formation of the polymer film.

1.4 DOPING

1.4.1 Doping and Undoping

Neutral conjugated polymers are not conductive. However, when they are oxidized or reduced, they become conductive. This process is called doping [1, 29-31]. After being doped, the polymer is positively or negatively charged. The anions or cations that neutralize this excess charge are called dopant ions or counter ions. The essence of doping is the oxidation or reduction of neutral polymer molecules to polycations or polyanions. A doped polymer can often be converted back to the neutral state. This process is called undoping. Even though undoping can be carried out both chemically and electrochemically, the electrochemical method is much easier.

1.4.2 Doping Methods

Doping can be carried out both chemically and electrochemically [29]. The chemical doping process is accomplished by exposing the polymer film to the vapour of the dopant, or by immersing the polymer film in a solution of the dopant. The amount of the dopant incorporated into the polymer depends on the vapour pressure of the dopant or its solution concentration, doping time, and temperature [29]. The electrochemical doping process can be carried out simply by applying a suitable potential to the polymer film in a common electrochemical cell. Electrochemically synthesized polymers are actually formed in the doped state as expressed by equation 1.1.

Electrochemical doping has the following advantages over chemical doping [32]: (1) the doping level can be easily controlled; (2) the approach to doping equilibrium can be determined by the current level; (3) the process is clean without formation of side products which require removal; and (4) the doping speed is generally much higher.

1.4.3 P-type Doping

When a polymer film is chemically doped by an electron acceptor, such as Br_2, I_2 or AsF_5, or when the polymer film is

doped through electrochemical oxidation, the polymer will lose electrons and the doped polymer film will have a positively charged backbone. This kind of doping is called p-type doping. Equations 1.4 and 1.5 are examples of the chemical and electrochemical p-type doping of polyacetylene, respectively.

$$(CH)_x + 3/2yI_2 \rightarrow (CH)_x^{y+} + yI_3^- \qquad (1.4)$$

$$(CH)_x + yClO_4^- -ye \rightleftharpoons [(CH)_x^{y+}(ClO_4^-)_y] \qquad (1.5)$$
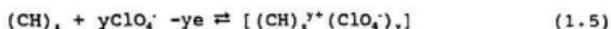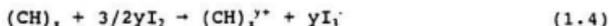
1.4.4 N-type Doping

When a polymer film is chemically doped by an electron donor, such as Li, Na, or K, or when the polymer film is doped through electrochemical reduction, the polymer will gain electrons. The resulting polymer has a negatively charged backbone, and the dopants are cations. This kind of doping is called n-type doping. Equations 1.6 and 1.7 are examples of the chemical and electrochemical n-type doping of polyacetylene, respectively.

$$(CH)_x + yLi \rightarrow (CH)_x^{y-} + yLi^+ \qquad (1.6)$$

$$(CH)_x + yLi^+ + ye \rightleftharpoons [(CH)_x^{y-}(Li^+)_y] \qquad (1.7)$$
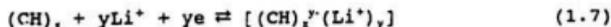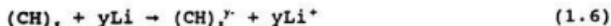
1.4.5 Self-Doping

A polymer that has a covalently bound dopant ion (counter ion) attached to its chain is a self-doped polymer. The bound ion must have an opposite charge to that of the oxidized or reduced polymer chains, and serves as an internal dopant ion. When the polymer is in the undoped state, the charge of the dopant ion is balanced by co-ions. When the polymer is oxidized or reduced, the co-ion moves out of the polymer to leave the covalently bound ion to balance the charge on the polymer chains. Therefore, it is the co-ion that moves into and out of the polymer film during the redox process. In view of its low electrochemical reactivity, the sulphonate group is usually chosen to serve as the covalently bound dopant ion for μ-type doping [33-36]. Equation 1.8 shows the self-doping process of the sodium salt of poly(thiophene ethanesulfonate) (P3-ETS) [36]. It is clear that sodium co-ion is the moving species during the redox process.

$$ (1.8) $$
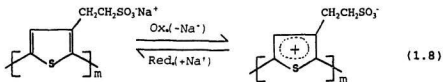
1.5 CONDUCTION MECHANISM

The conduction mechanism of conducting polymers is not fully understood. Since the neutral polymer film is not conductive until it is doped, and the conductivity increases with doping level, conduction must result from the formation of radical cations and dications [37-40] (Here conduction due to p-type doping is used as an example).

When an electron is removed from the top of the valence band of a conjugated polymer, a radical cation is created that does not delocalize completely [37, 38, 41], as would be expected. Only partial delocalization occurs, extending over several monomeric units. This radical cation has a spin of 1/2 and is called a polaron in the literature of conducting polymers. (Strictly, the term polaron refers to the wave-like disturbance or motion association with the electron in the conductance process). If the unpaired electron of a polaron is then removed, a dication or bipolaron is formed. The two positive charges of the bipolaron are not independent, but act as a pair, and a bipolaron is spinless [37, 38, 40, 41]. Usually, low doping levels give rise to polarons [42], and high doping levels produce bipolarons [43]. The presence of polarons has been detected in polypyrrole by ESR (electron
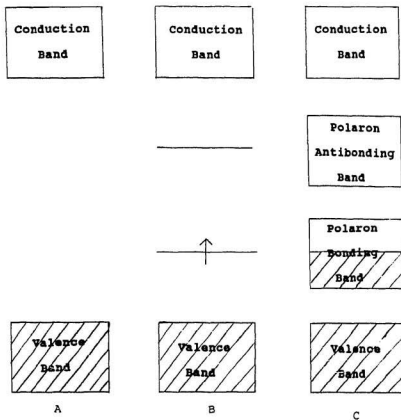
Fig.1.5. Evolution of the band structures upon doping of a conducting polymer: A--undoped; B--low doping level; and C--higher doping level.

spin resonance) and bands due to both polarons and bipolarons have been observed in optical experiments [43]. Both polarons and bipolarons are mobile and can move along polymer chains under the influence of an electric field. Therefore, the oxidized polymer is an electronic conductor.

Conduction due to the formation of polarons and bipolarons has also been treated using band theory [37, 38, 44-49]. According to band theory [50], only partially filled bands are responsible for conduction, and no conduction can take place if only empty and full bands exist. A metal is a material with a partially filled band so that it is a conductor. A semiconductor or an insulator differs from a metal in that its energy bands are either completely full or completely empty. In a semiconductor, conduction is possible when some electrons are promoted from the valence band to the conduction band to form partially filled bands. Whereas, an insulator has such a large band gap between the valence band and the conduction band that electrons can not be easily excited to the conduction band to create partially filled bands. It therefore can not conduct electricity.

Like an insulator, an undoped polymer has no partially filled bands, and the band gap is very large (Fig.1.5-A).

When it is oxidized, a polaron is formed. The removal of an electron from a bonding orbital results in an increase in the energy of this orbital, and a decrease in the energy of the corresponding antibonding orbital. Therefore, two new energy levels evolve from the orginal orbitals (Fig.1.5-B). At higher doping levels the polaron bonding and antibonding orbitals form two energy bands between the valence and conduction bands (Fig.1.5-C). Now a partially filled polaron bonding band is formed, and the energy difference between the valence band and the polaron antibonding band is smaller than the original band gap. Therefore, the conductivity is greatly enhanced, and the polymer is changed to a semiconductor or even a conductor from an insulator. When bipolarons are formed, a similar treatment can be used.

1.6 OVEROXIDATION

1.6.1 Overoxidation

Even though oxidation can change a conducting polymer from an insulating form to a conducting form, if the potential is too positive, an irreversible oxidation occurs. After this irreversible oxidation, the polymer is no longer conductive no matter how the potential is changed thereafter [51-61]. This deactivation of conducting polymers at high potential is

called overoxidation. Fig.1.6 shows cyclic voltammograms for
the reversible redox process and the overoxidation process of
poly(3-methylthiophene). Fig.1.6-A is the reversible redox
process observed when the potential is not taken higher than
1.0 V. This is a chemically reversible process, the anodic or
cathodic peak heights change very little during successive
potential scans. When the upper potential limit is too high,
however, a much larger anodic peak is observed at 1.9 V (curve
1'). No corresponding cathodic peak is observed on the
reverse scan and the cathodic peak of the reversible redox
process at about 0.7 V disappears. Subsequent scans show
negligible anodic and cathodic currents (curves 2' and 3').
Clearly, the polymer loses its conductivity during an anodic
scan to 2 V.

1.6.2 Mechanism

Overoxidation is believed to result from an attack by
nucleophilic species on the positively charged polymer. This
destroys the conjugation of the polymer chains so that the
overoxidized polymer becomes insulating. Since trace amounts
of water are always present in most of the solvents used,
water is thought to be the nucleophilic species in most cases
[52-54, 56, 57, 60, 61].
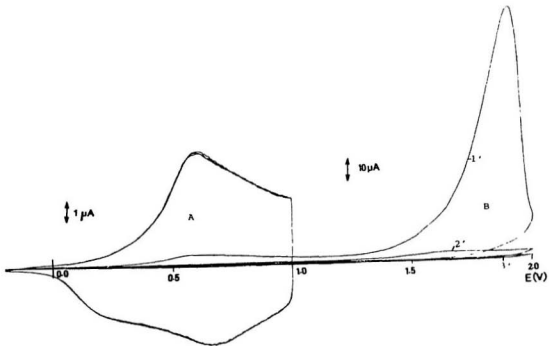
Fig.1.6. Cyclic voltammograms of a poly(3-methylthiophene) film (0.1 μm) in 0.1 M Et₄NClO₄/acetonitrile: A--chemically reversible redox process (consisting of three successive scans); and B--overoxidation process (1',2' and 3' are three successive scans). Scan rate = 100 mV/s.

The overoxidation process is not fully understood, but, the process expressed in Fig.1.7 is generally accepted [54, 57]. The first step is the radical cation (1) being further oxidized to the dication (2). This dication is very reactive and is attacked by a nucleophile such as water to yield a 3-hydroxy-pyrrole (3). The enol form (3) will be in equilibrium with a keto form (4), and both (3) and (4) can be oxidized to yield the pyrrolinone form (5). This pyrrolinone form may be further oxidized depending on the potential and nucleophiles. It is clear that after the attack by water on the dication, the polymer loses its conjugation. Then, the polymer is no longer conductive.

When a strong nucleophile such as OH⁻ is present, it has been proposed that it can initially add to the radical cation directly to form (6). Upon further oxidation, a ketone (7) is formed (Fig.1.8) [54]. In the presence of a weak nucleophile such as Br⁻, it was concluded that bromine substitution can occur, followed by carbonyl formation due to an attack by water (Eq.1.9) [54].

$$\left(\underset{\underset{H}{\big|}}{\boxed{}}\right)^{\overset{.}{+}}_m \xrightarrow[-5e^-,-5H^+]{Br^-, H_2O} \left(\underset{\underset{H}{\big|}}{\boxed{}}\right)_{m-1} \qquad (1.9)$$
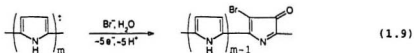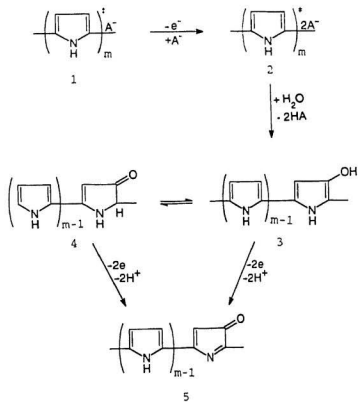
Fig.1.7. A generally accepted mechanism for the overoxidation of polypyrrole. m is the average chain length of a polaron or a bipolaron [54].
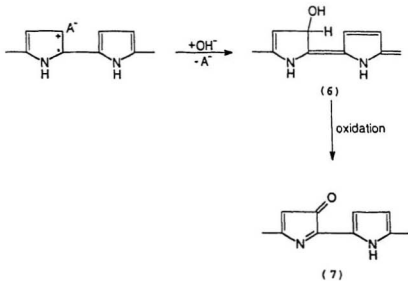
Fig.1.8. A mechanism for the overoxidation of polypyrrole in the presence of OH⁻ [54].

As studies on conducting polymers go further, more attention is being paid to the copolymerization of different monomer combinations. Copolymerization can result in better polymers or polymers with desired properties, such as higher stability [62-67] or higher solubility [68-71]. Copolymerization is an effective method to incorporate some functional groups into a conducting polymer. For example, through copolymerization of 3-methylthiophene and [Ru(bp)$_2$(pmp)$_2$]$^{2+}$, the later which is an oxidation catalyst, was incorporated into the conducting copolymer [72]. Copolymerization may also provide data for probing the structure/property relationships of conducting polymers [34, 66, 67, 73, 74]. And sometimes, copolymerization may help chemists understand the electrochemical polymerization mechanism [75].

Copolymers can be synthesized either chemically or electrochemically. If a copolymer possesses a redox potential intermediate to those of either homopolymer, it is usually a random copolymer [76]. On the other hand, if a copolymer shows two redox potentials, this implies the existence of two separate redox systems. Such a copolymer may contain either

27

a mixture of homopolymers, or may be a block copolymer [63].

It is a common experience that copolymerization can proceed at a potential lower than the value needed for the formation of the homopolymer with the highest polymerization potential. This may indicate that copolymerization can proceed via radical cation and neutral monomer coupling. Such a mechanism has actually been proposed by Wei et al [75]. By studying the electrochemical polymerization of thiophene, they found that the overall polymerization rate was significantly increased in the presence of bithiophene (or terthiophene), and the required potential could be reduced considerably to a value lower than the oxidation potential of thiophene monomer. The structure of the polymer formed was similar to that of polythiophene as indicated by FTIR (Fourier transform infrared) spectroscopy and cyclic voltammetry, but it was not similar to that of poly(2,2'-bithiophene). Based on these experimental results, they concluded that the polymerization proceeds via a radical cation and neutral monomer coupling mechanism, not a radical-radical coupling mechanism.

1.8 ELECTROCHEMISTRY OF CONDUCTING POLYMER COATED ELECTRODES

1.8.1 Cyclic Voltammetry

The redox process of a conducting polymer is very apparent when cyclic voltammetry of the film-coated electrode is studied [27]. During the anodic potential scan, an anodic peak appears due to the oxidation of the polymer film (Fig.1.8-A). As the potential is scanned back to its initial value, the oxidized polymer film is reduced and a cathodic peak is observed . A polymer film-coated electrode seldom shows identical anodic and cathodic peaks [77]. The average of the anodic and cathodic peak potentials, $E^{o'}$, which is an important characteristic of a conducting polymer, is called the apparent formal potential.

In order to maintain the electroneutrality of the whole polymer film, cations or anions are involved in the redox process. For example, anions from the supporting electrolyte may move into the film during the oxidation process, or cations initially present in the polymer film may move out. The transport rates of these ions determine how fast a conducting polymer can be oxidized or reduced. If the rate is fast, or the polymer film is sufficiently thin, or the scan rate is slow enough, the whole polymer film behaves like a

monolayer, and the peak current i_p is proportional to the scan rate ν [77].

1.8.2 Electrostatic Binding and Ionic Conducting Polymers

When an electrode is coated with an ionic conducting polymer film [78-82], the film has the ability to concentrate charged electroactive species from the supporting electrolyte through electrostatic binding even when it is in the undoped state. This is actually an ion exchange process. The counter ion initially present in the film is replaced by the electroactive species. The concentration of the charged sites in the film can be as high as 5 M [78]. This high concentration is preferable in microanalysis and catalysis [77]. For example, the high anion exchange capacity of poly(1-methyl-3-(pyrrol-1-ylmethyl)pyridinium) has been used to preconcentrate $Fe(CN)_6^{3/4-}$ as a mediator for ascorbic acid oxidation [78].

Similar to the polymer film, the electroactive species will be reduced and oxidized when the potential is scanned. Even though it is not always clear how charge is transported in a polymer containing mobile electroactive species [77]: by physical diffusion of the electroactive species [83], or by electron hopping between the electroactive species [84], it

30

has been found that the charge transport rate obeys diffusion laws [85-87]. Therefore, it can be expressed mathematically by a charge transport diffusion coefficient D_{ct}. The concentration profiles of the two forms of the electroactive couple depend on the parameter $D_{ct}\tau/d^2$, where τ is the experimental time scale and d is the thickness of the film. If $D_{ct}\tau/d^2 \ll 1$, only the species near the electrode-polymer interface will be changed, and that near the polymer-solution interface will be unaffected by the experiment. This means that the semi-infinite diffusion condition prevails. Therefore, all electrochemical relationships derived for semi-infinite diffusion conditions are valid for a polymer coated electrode. For example, the cyclic voltammetric peak current, I_p, is proportional to $v^{1/2}$ and the Randles-Sevcik equation is valid [85, 88]:

$$I_p = 2.69\text{x}10^5 n^{3/2} A D_{ct}^{1/2} v^{1/2} C_p \qquad (1.10)$$

where A is the area of the polymer film, v the scan rate, and C_p the concentration of the electroactive species in the film.

1.9 OBJECTIVE AND OUTLINE OF THIS THESIS

Even though poly(1-methyl-3-(pyrrol-1-ylmethyl)

31

pyridinium) (poly-MPMP$^+$) has a higher ionic conductivity than polypyrrole [89], its electronic conductivity [90] is much lower than that of either polypyrrole or polythiophene. Since a copolymer usually possesses intermediate properties between the homopolymers, the copolymerization of MPMP$^+$ with 3-methylthiophene (MeTh) was carried out, with the goal to increase the electronic conductivity while keeping the higher ionic conductivity and better ion-exchange properties of poly-MPMP$^+$. The desired MeTh-MPMP$^+$ copolymers were electrochemically synthesized. The experimental details, along with some important conclusions, are discussed in chapter 3.

When poly(MeTh$_x$-MPMP$^+$) films were studied in aqueous K_2HPO_4 containing $K_3Fe(CN)_6$, it was found that the anodic to cathodic peak height ratio was about 1:1 at high scan rates, but decreased to 0.75:1 at low scan rates. Moreover, the electrochemical response of $Fe(CN)_6^{3-/4-}$ within the copolymer began to decrease after saturation, and after several hours, the voltammetric peaks nearly disappeared. Since these two phenomena may occur when other ionic conducting polymer films are studied in the same solution or in a solution containing other electroactive species, this study is believed to have general application. Chapters 4 and 5 are about these two

phenomena.

Although the problem of overoxidation has been known since the very early work of Diaz et al [51], chemists have not found any method to reactivate overoxidized polymers. The challenge of this problem allured us to do some work in this area. After some exploratory research, we found two methods to reactivate poly(3-methylthiophene) that had been overoxidized in the presence of Cl⁻. We also discovered an interesting electrochemical substitution reaction with both Cl⁻ and Br⁻. These discoveries will further chemists' understanding of the overoxidation mechanism, and should stimulate further studies.

REFERENCES

1. H. Shirakawa, E.J. Louis, A.G. MacDiarmid, C.K. Chiang, and A.J. Heeger, *J. Chem. Soc.*, *Chem. Commun.*, 578 (1977).

2. V.V. Walatka, M.M. Labes, and J.H. Perlstein, *Phys. Rev. Lett.* **31**, 1139 (1973).

3. A.F. Diaz, K.K. Kanazawa, and G.P. Gardini, *J. Chem. Soc.*, *Chem. Commun.*, 635 (1979).

4. D.M. Ivory, G.G. Miller, J.M. Sowa, L.W. Shacklette, R.R. Chance, and R.H. Baughman, *J. Chem. Phys.* **71**, 1506 (1979).

5. G.E. Wnek, J.C.W. Chien, F.E. Karasz, and C.P. Lillya, *Polymer* **20**, 1441 (1979).

6. J.F. Rabolt, T.C. Clarke, K.K. Kanazawa, J.R. Reynolds, and G.B. Street, *J. Chem. Soc.*, *Chem. Commun.*, 347 (1980).

7. R.R. Chance, L.W. Shacklette, G.G. Miller, D.M. Ivory, J.M. Sowa, R.L. Elsenbaumer, and R.H. Baughman, *J. Chem. Soc.*, *Chem. Commun.*, 348 (1980).

8. T. Yamamoto, K. Saneckika, and A. Yamamoto, *J. Polym. Sci. Polym. Letter. Ed.* **18**, 9 (1980).

9. T.A. Skotheim, Ed., *Handbook of Conducting Polymers*, vol. 1 & 2 (Marcel Dekker, New York and Basel, 1986).

10. W.J. Feast, in *Handbook of Conducting Polymers*, vol. 1, T.A. Skotheim, Ed. (Marcel Dekker, New York and Basel, 1986), pp. 1-43.

11. J. Bargon, S. Mohmand, and R.J. Waltman, *IBM J. Res. Dev.* **27**, 330 (1983).

12. R.J. Waltman and J. Bargon, *Can. J. Chem.* **64**, 76 (1986).

13. A.F. Diaz and J. Bargon, in *Handbook of Conducting Polymers*, vol. 1, T.A. Skotheim, Ed. (Marcel Dekker, New York and Basel, 1986), pp. 81-115.

14. G.B. Street, in *Handbook of Conducting Polymers*, vol. 1,

T.A. Skotheim, Ed. (Marcel Dekker, New York and Basel, 1986), pp. 265-291.

15. T. Inoue and T. Yamase, *Bull. Chem. Soc. Jpn.* **56**, 985 (1983).

16. E.M. Genies, G. Bidan, and A.F. Diaz, *J. Electroanal. Chem.* **149**, 101 (1983).

17. C.P. Andrieux, P. Audebert, P. Hapiot, and J.M.Savèant, *J. Phys. Chem.* **95**, 10158 (1991).

18. A.F. Diaz, J. Crowley, J. Bargon, G.P. Gardini, and J.B. Torrance, *J. Electroanal. Chem.* **121**, 355 (1981).

19. R.N. Adams, *Acc. Chem. Res.* **2**, 175 (1969).

20. R.J. Waltman and J. Bargon, *Tetrahedron* **40**, 3963 (1984).

21. B.R. Scharifker, E. Garcia-Pastoriza, and W. Marino, *J. Electroanal. Chem.* **300**, 85 (1991).

22. A.F. Diaz, A. Martinez, K.K. Kanazawa, and M. Salmon, *J. Electroanal. Chem.* **130**, 181 (1981).

23. G.P. Gardini, *Adv. Heterocycl.Chem.* **15**, 95 (1973).

24. G.B. Street, T.C. Clarke, M. Krounbi, K. Kanazawa, V. Lee, P. Pfluger, J.C. Scott, and G. Weiser, *Mol. Cryst. Liq. Cryst.* **83**, 253 (1982).

25. G.B. Street, T.C. Clarke, G.H. Geiss, V.Y. Lee, P. Pfluger, and J.C. Scott, *J.Phys.Colloq.* **C3**, 599 (1983).

26. J.A. Pople and D.L. Beveridge, Eds., *Approximate Molecular Orbital Theory* (McGraw-Hill, New York, 1970).

27. J. Heinze, *Synth. Met.* **41-43**, 2805 (1991).

28. M. Kaneko and D. Wöhrle, in *Advances in Polymer Sciences*, Vol. 84 (Springer-Verlag, Berlin and heidelberg, 1988), pp 141-228.

29. M. Aldissi, Ed., *Inherently Conducting Polymers: Processing, Fabrication, Applications, Limitations* (Noyes Data Corporation, New Jersey, 1989), pp. 40-48.

30. C.K. Chiang, M.A. Druy, S.C. Gau, A.J. Heeger, E.J.

Louis, A.G. MacDiarmid, Y.W. Park, and H. Shirakawa, *J. Am. Chem. Soc.* **100**, 1013 (1978).

31. C.K. Chiang, J. Fincher CR, Y.W. Park, A.J. Heeger, H. Shirakawa, E.J. Louis, S.C. Gau, and A.G. MacDiarmid, *Phys. Rev. Lett.* **39**, 1098 (1977).

32. J.R. Ferraro and J.M. Williams, Eds., *Introduction to Synthetic Electrical Condutors* (Academic Press, Florida, 1987), pp. 92.

33. A.O. Patil, Y. Ikenoue, N. Basescu, N. Colaneri, J. Chen, F. Wudl, and A.J. Heeger, *Synth. Met.* **20**, 151 (1987).

34. J.R. Reynolds, N.S. Sundaresan, M. Pomerantz, S. Basak, and C.K. Baker, *J. Electroanal. Chem.* **250**, 355 (1988).

35. N.S. Sundaresan, S. Basak, M. Pomerantz, and J.R. Reynolds, *J. Chem. Soc., Chem. Commun.*, 621 (1987).

36. Y. Ikenoue, J. Chiang, A.O. Patil, F. Wudl, and A.J. Heeger, *J. Am. Chem. Soc.* **110**, 2983 (1988).

37. J.L. Bredas, R.R. Chance, and R. Silbey, *Mol. Cryst. Liq. Cryst.* **77**, 319 (1981).

38. J.L. Bredas, R.R. Chance, and R. Silbey, *Phys. Rev. B:. Condens. Matter.* **26**, 5843 (1982).

39. D.S. Boudreaux, R.R. Chance, J.L. Bredas, and R. Silbey, *Phys. Rev. B:. Condens. Matter.* **28**, 6927 (1983).

40. R.R. Chance, D. Boudreaux, J.L. Bredas, and R. Silbey, in *Handbook of Conducting Polymers*, vol. 2, T.A. Skotheim, Ed. (Marcel Dekker, New York and Basel, 1986), pp. 825-857.

41. J.L. Bredas, J.C. Scott, K. Yakushi, and G.B. Street, *Phys. Rev. B:. Condens. Matter.* **30**, 1023 (1984).

42. R.L. Greene and G.B. Street, *Science.* **226**, 651 (1984).

43. J.C. Scott, J.L. Bredas, K. Yakushi, P. Pfluger, and G.B. Street, *Synth. Met.* **9**, 165 (1984).

44. J.L. Bredas, in *Handbook of conducting polymers*, vol. 2, T.A. Skotheim, Ed. (Marcel Dekker, New York and Basel, 1986), pp. 859-913.

45. E.J. Mele and M.J. Rice, *Phys. Rev. B:. Condens. Matter.* **23**, 5397 (1981).

46. J.L. Bredas, B. Themans, and J. Andre, *Phys. Rev. B:. Condens. Matter.* **27**, 7827 (1983).

47. J.L. Bredas, R.R. Chance, R. Silbey, G. Nicolas, and P. Durand, *J. Chem. Phys.* **75**, 255 (1981).

48. J.L. Bredas, R.R. Chance, R.H. Baugh man, and R. Silbey, *J. Chem. Phys.* **76**, 3673 (1982).

49. J.L. Bredas, R.L. Elsenbaumer, R.R. Chance, and R. Silbey, *J. Chem. Phys.* **78**, 5656 (1983).

50. A.J. Epstein and J.S. Miller, *Sci.Am.* **241**, 52 (1979).

51. A.F. Diaz, J.I. Castillo, J.A. Logan, and W.Y. Lee, *J. Electroanal. Chem.* **129**, 115 (1981).

52. P.A. Christensen and A. Hamnett, *Electrochimica Acta* **36**, 1263 (1991).

53. F. Beck and A. Pruss, *J. Electroanal. Chem.* **216**, 157 (1987).

54. F. Beck, P. Braun, and M. Oberst, *Ber. Bunsenges. Phys. Chem.* **91**, 967 (1987).

55. B. Krische and M. Zagorska, *Synth. Met.* **28**, C263 (1989).

56. G. Horanyi and G. Inzelt, *J. Electroanal. Chem.* **257**, 311 (1988).

57. F. Beck, P. Braun, and Schloten, *J. Electroanal. Chem.* **267**, 141 (1989).

58. A. Witkowski, M.S. Freund, and A. Brajter-Toth, *Anal. Chem.* **63**, 622 (1991).

59. M. Gratzl, D.F. Hsu, A.M. Riley, and J. Janata, *J. Phys. Chem.* **94**, 5973 (1990).

60. E.W. Tsai, S. Basak, J.P. Ruiz, J.R. Reynolds, and K. Rajeshwar, *J. Electrochem. Soc.* **136**, 3683 (1989).

61. P. Novak, B. Rasch, and W. Vielstich, *J. Electrochem. Soc.* **138**, 3300 (1991).

62. S. Kuwabata, S. Ito, and H. Yoneyama, *J. Electrochem. Soc.* **135**, 1691 (1988).

63. P. Novak and W. Vielstich, *J. Electroanal. Chem.* **300**, 99 (1991).

64. T. Iyoda, H. Toyoda, M. Fujitsuka, R. Nakahara, H. Tsuchiya, K. Honda, and T. Shimidzu, *J. Phys. Chem.* **95**, 5215 (1991).

65. K. Naoi, T. Hirabayashi, I. Tsubota, and T. Osaka, *Bull. Chem. Soc. Jpn.* **60**, 1213 (1987).

66. M.S. Kiani and G.R. Mitchell, *Synth. Met.* **46**, 293 (1992).

67. W. Torres and M.A. Fox, *Chem. Mater.* **4**, 146 (1992).

68. Z. Yang and H.J. Geise, *Synth. Met.* **47**, 95 (1992).

69. M. Aldissi, *J. Chem. Soc., Chem. Commun.*, 1347 (1984).

70. P. Kathirgamanathan, P.N. Adams, K. Quill, and A.E. Underhill, *J. Mater. Chem.* **1**, 141 (1991).

71. H.S. Nalwa, *Synth. Met.* **35**, 387 (1990).

72. J. Ochmanska and P.G. Pickup, *Can. J. Chem.* **69**, 653 (1991).

73. J.P. Montheard, G. Boiteux, B. Themans, J.L. Bredas, T. Pascal, and G. Froyer, *Synth. Met.* **36**, 195 (1990).

74. C. Mailhe-Randolph and A.J. McEvoy, *Ber. Bunsenges. Phys. Chem.* **93**, 905 (1989).

75. Y. Wei, C.C. Chan, J. Tian, G.W. Jang, and K.F. Hsueh, *Chem. Matar.* **3**, 888 (1991).

76. K.K. Kanazawa, A.F. Diaz, M.T. Krounbi, and G.B. Street, *Synth. Met.* **4**, 119 (1981).

77. R.W. Murray, in *Electroanalytical Chemistry*, vol. 13, A.J. Bard, Ed. (Marcel Dekker, New York and Basel, 1984), pp. 191-368.

78. H. Mao and P.G. Pickup, *J. Electroanal. Chem.* **265**, 127 (1989)

79. S. Cosnier, A. Deronzier, J.-C. Moutet and J.F. Roland, *J. Electroanal. Chem.* **271**, 69 (1989).

80. P.N. Bartlett, L.-Y. Chung, and P. Moore, *Electrochimica Acta.* **35**, 1273 (1990).

81. B. Keita, D. Bouaziz, and L. Nadjo, *J. Electroanal. Chem.* **279**, 187 (1990).

82. T. Iyoda, M. Aiba, T. Saika, K. Honda, and T. Shimidzu, *J. Chem. Soc. Faraday Trans.* **87**, 1765 (1991).

83. K. Doblhofer and R.D. Armstrong, *Electrochimica Acta.* **33**, 453 (1988).

84. F.B. Kaufman, A.H. Schroeder, E.M. Engler, S.R. Kramer, and J.Q. Chambers, *J. Am. Chem. Soc.* **102**, 483 (1980).

85. P. Daum, J.R. Lenhard, D. Rolison, and R.W. Murray, *J. Am. Chem. Soc.* **102**, 4649 (1980).

86. R.J. Nowak, F.A. Schultz, M. Umana, R. Lam, and R.W. Murray, *Anal. Chem.* **52**, 315 (1980).

87. N. Oyama and F.C. Anson, *J. Electrochem. Soc.* **127**, 640 (1980).

88. A.J. Bard and L.R. Faulkner, Eds., *Electrochemical Methods-Fundamentals and Applications* (John Wiley & Sons, New York, 1980), pp.213-248.

89. H. Mao and P.G. Pickup, *J. Phys. Chem.* **93**, 6480 (1989).

90. H. Mao and P.G. Pickup, *J. Am. Chem. Soc.* **112**, 1776 (1990).

Chapter 2 EXPERIMENTAL

2.1 ELECTROCHEMISTRY

Electrochemical experiments were carried out in conventional three compartment glass cells at 23 ± 2 °C. The solution was purged with argon prior to voltammetric studies, but not for polymer preparation nor ion-exchange. A 0.0052 cm² Pt disc sealed in glass was used as working electrode unless otherwise stated. Each working electrode was polished with 0.3 μm alumina on a polishing cloth before each experiment. A Pt wire was used as the counter electrode, and a saturated sodium chloride calomel electrode (SSCE) was used as the reference electrode, except for AC impedance measurements, where a Ag/AgCl/0.1 M Cl⁻ (aq) electrode with a 0.1 M Et₄NClO₄ (aq.) salt bridge was used as the reference electrode. This reference electrode had a potential of +70 mV vs. SSCE. All potentials were quoted with respect to the SSCE reference electrode.

Voltammetric measurements were made using a Pine Instruments RDE4 potentiostat/galvanostat and a BBC SE 780 X-Y recorder. AC impedance measurements were performed using a Solartron 1286 electrochemical interface and a Solartron 1250

frequency response analyzer. All data were collected and
analyzed using ZPLOT software (Scribner Associates Inc.) on a
Laser 286-M microcomputer. The sine-wave amplitude was 5 mV
RMS for all experiments.

2.2 CHEMICALS

1-methyl-3-(pyrrol-1-ylmethyl) pyridinium
tetrafluoroborate (MPMPBF$_4$) was synthesized as previously
described [1]. 4-chlorobenzenesulfonic acid (Tech.90%) was
purified by recrystallization from benzene. 3-methylthiophene
(Aldrich,99%), tetraethylammonium perchlorate (Et$_4$NClO$_4$,
Fluka,>99%), acetonitrile (Fisher,HPLC grade), sodium
2-chloroethanesulfonate (Aldrich), poly(4-vinylpyridine)
(Polysciences), p-toluenesulphonic acid (The British Drug
Houses Ltd.,98%), 2,3-dichloro-5,6-dicyano-1,4-benzoquinone
(Aldrich), and other chemicals were used as received.

2.3 PREPARATION OF POLY-MPMP$^+$

Poly-MPMP$^+$ films were synthesized from acetonitrile
containing 0.05 M MPMP$^+$ + 0.1 M Et$_4$NClO$_4$ at a current density
of 0.77 mA/cm^2. A charge density of 0.15 C/cm^2 was assumed to
produce a 1.0 μm thick polymer film [1].

2.4 SCANNING ELECTRON MICROSCOPY

A Hitachi S-570 scanning electron microscope was used to examine morphologies of copolymers. A small piece of copper foil was wrapped tightly on the conductive side of an indium/tin oxide coated glass slide (Donnelly Corp., 10 $\Omega/\square$) with a piece of adhesive tape to give a good contact. The tape was then covered with epoxy (Epoxi-Patch, Dexter Corp.). The actual area of the glass slide was measured under a linear vernier microscope. After a copolymer film was generated on the glass slide, the slide was broken along a slot cut on its non-conductive side. The polymer, along with the glass slide, was covered by a thin gold film to prevent charging when the morphology of the polymer film was studied using the scanning electron microscope.

2.5 X-RAY EMISSION ANALYSIS

The composition of a polymer is usually determined by elemental analysis. However, this method can not be used to measure directly the composition of a thin polymer film deposited on an electrode. It was therefore important in this work to develop a rapid, non-destructive method to analyze thin polymer films on small electrodes.

42

Energy dispersive x-ray analysis has been successfully applied to the analysis of small poly(MeTh$_x$-MPMP$^+$) films. The fully reduced copolymer contains ClO$_4^-$ only as the counter ion to balance the permanent positive charge of MPMP$^+$ units, and so the ClO$_4^-$:MPMP$^+$ ratio should be 1:1 (Fig.2.1). Therefore, the atomic ratio of sulphur to chlorine, S:Cl, which can be obtained from x-ray analysis, represents the average ratio of MeTh to MPMP$^+$ in the copolymer.

X-ray analysis was performed with a Tracor Northern 5500 Energy Dispersive X-ray Analyzer associated with the scanning electron microscope. Relative elemental concentrations were estimated using Tracor Northern's software package—"SQ"—Standardless Quantitative Analysis. This program provides rapid, easy and standardless analysis of x-ray spectra acquired from a bulk specimen. It removes background, extracts peak areas, calculates normalized intensity ratios and corrects for matrix effects. ZAF is the theoretical program for the correction of matrix effects. ZAF can automatically correct for the influences arising from the atomic number (Z), absorption (A) and fluorescence (F) of each element. It then displays these correction factors, the total correction factor, and the atomic fraction and weight fraction for each element.
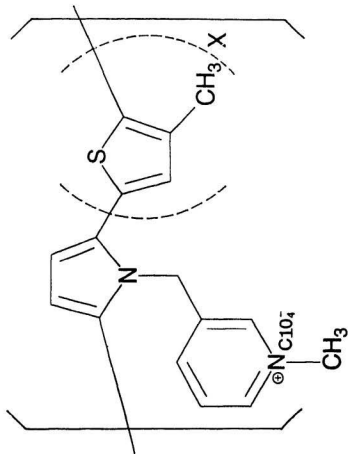
Fig.2.1. A proposed structure of poly(MeTh,-MPMP').

Even though the analyzer was programmed to take as many factors as possible into consideration, it was still thought necessary to calibrate the analysis. The method was calibrated by analyzing polymers and coatings of known S and Cl contents. Firstly, 0.4 μm thick poly-MPMP$^+$ClC$_2$H$_4$SO$_3^-$ films deposited on glassy carbon (Electrosynthesis Corp.) electrodes of 0.0707 cm^2 sealed in glass with epoxy (Lepage's) were used. Poly-MPMP$^+$ClO$_4^-$ films were first synthesized and then fully reduced at about -0.2 V. They were immersed in a stirred methanol solution containing 0.4 M sodium 2-chloroethanesulfonate (ClC$_2$H$_4$SO$_3$Na) so that ClO$_4^-$ would be replaced by ClC$_2$H$_4$SO$_3^-$. Assuming that all of the ClO$_4^-$ counter ions were replaced by ClC$_2$H$_4$SO$_3^-$, the polymers would have contained equal amounts of S and Cl atoms. This assumption was proved valid if the solution was stirred for about 15 minutes. However, the analyzed average S:Cl ratio of three measurements was 51.6:48.4. Therefore, each S:Cl ratio should be corrected by a factor of 0.94 ($\pm$ 0.02). Fig.2.2 shows the x-ray emission spectrum of a reduced poly-MPMP$^+$ClC$_2$H$_4$SO$_3^-$ film.

Secondly, two different known composition coatings with S:Cl ratios of 1:1 and 2:1 prepared from mixtures of 4-chlorobenzenesulfonic acid (ClC$_6$H$_4$SO$_3$H) and p-toluenesulphonic acid (CH$_3$C$_6$H$_4$SO$_3$H.H$_2$O) were used. In order to simulate the

45
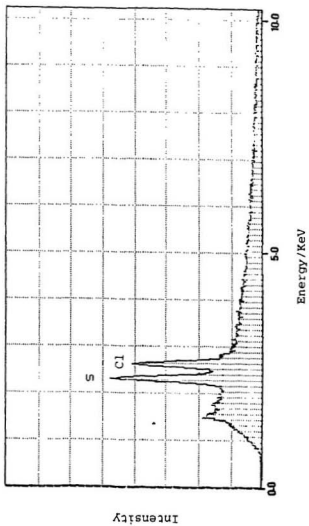
Fig.2.2. X-ray emission spectrum of a reduced poly-MPMP⁺Cl/C₆H₄SO₃⁻ film. The parent poly-MPMP⁺ film was generated on a 0.0707 cm² carbon electrode at a current density of 0.77 mA/cm² from 0.05 M MPMP⁺/acetonitrile.
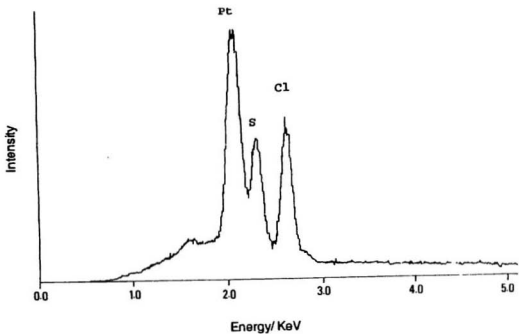
Fig.2.3. X-ray emission spectrum of a 3.0 μm thick poly(MeTh₄-MPMP⁺) film deposited on a Pt electrode. The copolymer was prepared at a current density of 7.7 mA/cm² from acetonitrile containing 0.01 M MPMP⁺ + 0.1 M MeTh + 0.1 M Et₄NClO₄.

matrix and composition of the copolymers, and to make the coatings more homogeneous and adherent to the carbon electrode surfaces, poly(4-vinylpyridine) (PVP) was added to their methanol solutions. The solution with the S:Cl ratio of 1:1 contained 5 M $ClC_6H_4SO_3H$ and 5 M PVP; while the solution with the S:Cl ratio of 2:1 contained 0.60 M $ClC_6H_4SO_3H$, 0.60 M $CH_3C_6H_4SO_3H.H_2O$ and 1.2 M PVP. Each coating was prepared by pipetting about 15 μl of solution onto a carbon electrode surface. After x-ray analysis was performed, a correction coefficient of 0.95 ($\pm$ 0.04) for the S:Cl ratio was obtained. Since the correction coefficients obtained from these two methods were in good agreement, S:Cl ratios were corrected by a factor of 0.94 in this work.

If copolymers are deposited on Pt electrodes for x-ray emission analysis, the copolymer films must be thick enough to suppress the Pt peak. This Pt peak is near the S peak (Fig.2.3) and could interfere with the results. It was found that the presence of a large Pt peak diminishes the apparent MeTh:$MPMP^+$ ratio. However, when a copolymer is thicker than 1 μm, even though the Pt peak may still be quite large, which means that x-rays can still go through the copolymer to strike the Pt surface, the presence of Pt does not significantly interfere with the x-ray analysis results.

If a copolymer film thinner than 1 μm must be analyzed, a carbon electrode should be used. The estimation of film thickness is discussed in section 3.2.5.

2.6 CONDUCTIVITY MEASUREMENTS

2.6.1 In Situ Dual Electrode Method

A dual electrode assembly consists of two electrodes sealed separately in one glass rod (Fig.2.4) [2, 3]. After a polymer film was generated on one of the two electrodes, the whole glass surface including the two Pt disc electrodes was covered with a thin gold film by vacuum deposition. The gold film was porous enough to allow the ions and solvent to move into and out of the polymer film freely. During the measurement, the whole sandwich electrode assembly was immersed in 0.1 M Et$_4$NClO$_4$/acetonitrile. Two potentials with a small difference, ΔE_{Pt-Au} (10 - 30 mV), were exerted on the polymer coated Pt electrode and the bare Pt electrode respectively. The potential applied to the polymer film could be viewed as the average of the two potentials. Since the polymer's electronic resistance is usually much higher than that of the gold film, the small potential difference ΔE_{Pt-Au} could be assumed to be the potential drop across the polymer film.
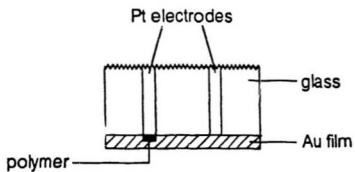
Fig.2.4. Cross section of a dual electrode assembly.

This potential difference resulted in a current, I_E, flowing through the polymer film. Therefore, the polymer's electronic conductivity at any potential E, $\sigma(E)$, can be calculated using the following equation:

$$\sigma(E) = (I_E d)/(\Delta E_{R,Av} A) \qquad (2.1)$$

Where d and A are the thickness and area of the polymer film, respectively.

2.6.2 AC Impedance Method

The AC impedance technique has been widely used to measure charge-transport processes in conducting polymers [4]. AC impedance data for a conducting polymer are conveniently analyzed using Nyquist plots as shown in Fig.2.5. The real-axis intercepts for the bare Pt electrode and the reduced polymer coated electrode, A and B, represent the solution resistance (R_s) and the sum of R_s and the reduced polymer's ionic resistance ($R_{i,Red}$), respectively [5]. From the difference, B-A, and the thickness and area of the polymer film, the ionic conductivity of the reduced polymer film can be calculated. The Nyquist plot of the oxidized polymer coated electrode should consist of distinct high-frequency and low-frequency parts at 45° and 90° to the real-axis
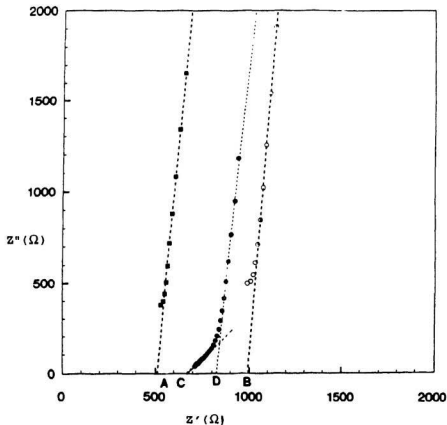
Fig.2.5. Imaginary impedance (Z") versus real impedance (Z')
plots for a bare Pt electrode, and a poly(MeTh,-MPMP⁺) coated
Pt electrode at 0.07 V and 0.92 V in 0.1 M Et₄NClO₄/
acetonitrile.   The copolymer (2.5 μm) was generated from
acetonitrile containing 0.01 M MPMP⁺ + 0.2 M MeTh + 0.1 M
Et₄NClO₄ at a current density of 0.77 mA/cm².

respectively [6, 7]. The high-frequency intercept, obtained by drawing a 45° tangent through the high-frequency part, gives $R_s + R_\infty$ (point C), where [6, 7]

$$1/R_\infty = 1/R_E + 1/R_I \qquad (2.2)$$

The low-frequency intercept, obtained by extrapolating the low frequency part, gives $R_s + R_t/3$ (point D), where [6, 7]

$$R_t = R_E + R_I \qquad (2.3)$$

(R_E and R_I represent the electronic and ionic resistance of the oxidized polymer film, respectively). From equations 2.2 and 2.3, R_E and R_I can be calculated, and they were distinguished based on comparisons with dual electrodes results and the expectation that R_I and $R_{I,Red}$ would be similar.

2.7 DIFFUSION COEFFICIENT MEASUREMENTS BY CHRONOAMPEROMETRY

As mentioned in section 1.8.2, charge transport in polymer films obeys diffusion laws, and when $D_p\tau/d^2 \ll 1$, the semi-infinite diffusion condition prevails. Therefore, for a potential step experiment the decay of current should follow the Cottrell equation [8, 9]:

$$I = (nFAD_p^{1/2}C_p) / (\pi^{1/2}t^{1/2}) \qquad (2.4)$$

where F is the Faraday constant, C_p and D_p are the
concentration and diffusion coefficient of the electroactive
species in the polymer film respectively, t is the time
counted from the potential step. If C_p is known, D_p can be
calculated from the slope of an $I-t^{1/2}$ plot. This is the
theoretical basis for measuring the diffusion coefficient of
an electroactive species in a polymer film by
chronoamperometry. If the film thickness is known, C_p can be
estimated according to the area under a cyclic voltammogram
recorded at a slow scan rate . The equation used to estimate
C_p is:

$$C_p = 10^3 Q_{cv} / (nFAd) \qquad (2.5)$$

where Q_{cv} is the voltammetric charge.

REFERENCES

1. H. Mao and P.G. Pickup, *J. Electroanal. Chem.* **265**, 127 (1989).

2. P.G. Pickup, W. Kutner, C.R. Leidner, and R.W. Murray, *J. Am. Chem. Soc.* **106**, 1991 (1984).

3. J. Ochmanska and P.G. Pickup, *J. Electroanal. Chem.* **297**, 211 (1991).

4. M.M. Musiani, *Electrochimica Acta*, **35**, 1665 (1990).

5. P.G. Pickup, *J. Chem. Soc., Faraday Trans.* **86**, 3631 (1990).

6. W.J. Albery, Z. Chen, B.R. Horrocks, A.R. Mount, P.J. Wilson, D. Bloor, A.T. Monkman, and C.M. Elliott, *Faraday Discuss. Chem. Soc.* **88**, 247 (1989).

7. W.J. Albery, C.M. Elliott, and A.R.Mount, *J. Electroanal. Chem.* **288**, 15 (1990)

8. P. Daum, J.R. Lenhard, D. Rolison, and R.W. Murray, *J. Am. Chem. Soc.* **102**, 4649 (1980).

9. A.J. Bard and L.R. Faulkner, Eds., *Electrochemical Methods-Fundamentals and Applications* (John Wiley & Sons, New York, 1980), pp.136-212.

Chapter 3   COPOLYMERIZATION OF 3-METHYLTHIOPHENE

WITH 1-METHYL-3-(PYRROL-1-YLMETHYL)PYRIDINIUM AND

CHARACTERIZATION OF COPOLYMER FILMS

3.1   INTRODUCTION

Its high ionic conductivity and high concentration of permanent positively charged sites make poly(1-methyl-3-(pyrrol-1-ylmethyl))pyridinium (poly-MPMP⁺) a very attractive conducting polymer [1, 2]. It would be even more attractive if its electronic conductivity [3, 4] could be increased. Since polythiophene and its derivatives have higher electronic conductivities [5-10], the electrochemical copolymerization of MPMP⁺ with 3-methylthiophene (MeTh) was carried out, with the goal to generate an ionic polymer with higher electronic conductivity. This study has led to several important conclusions concerning oxidation level, morphology, composition, and electronic and ionic conductivities of MeTh-MPMP⁺ copolymers. Also, x-ray emission analysis was developed as a rapid and non-destructive method to analyze the compositions of the copolymers, and to determine the oxidation levels of poly(3-methylthiophene) and the copolymers. This chapter reports these experimental results in detail.

3.2 RESULTS

3.2.1 Preparation of Copolymers

Poly(MeTh,-MPMP⁺) could be generated from a wide compositional range of monomer solutions. When galvanostatic polymerization was employed, a current density higher than 0.65 mA/cm^2 was required. When copolymers were prepared potentiostatically, the proper potential was between 1.2 V and 1.5 V. Comparatively, the best potential range for preparing poly-MPMP⁺ was 1.1 V to 1.2 V, while 3-methylthiophene could not be polymerized at potentials smaller than 1.43 V.

3.2.2 Composition of Copolymers

Compositions from x-ray analysis of copolymers prepared galvanostatically under different conditions and then reduced are shown in Fig.3.1. The MeTh:MPMP⁺ ratio in the copolymers increases as the current density increases, or as the MeTh:MPMP⁺ ratio in the monomer solution is increased. There are linear relationships between current density and the percentage of MeTh in the copolymer for monomer solutions with the MeTh:MPMP⁺ ratio up to at least 100:1 (curves A,B and C). However, above a certain current density, and for monomer solutions containing less MPMP⁺, the composition of the copolymer is not strongly correlated with current density
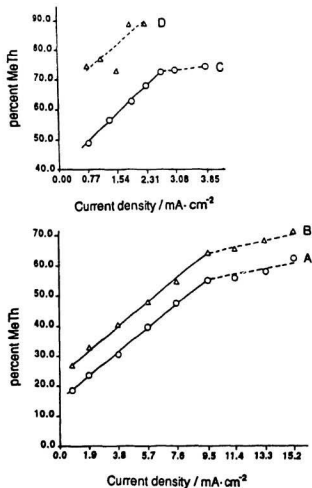
Fig.3.1. Compositions of copolymers produced galvanostatically from different monomer solutions containing 0.1 M Et$_4$NClO$_4$/acetonitrile: A--0.01 M MPMP$^+$ + 0.1 M MeTh; B--0.01 M MPMP$^+$ + 0.2 M MeTh; C--0.002 M MPMP$^+$ + 0.2 M MeTh; and D--0.5 mM MPMP$^+$ + 0.2 M MeTh.

(curve D and the dashed line parts of curves A,B and C).
Curve D is only an illustrative group of experimental results.

3.2.3 Determination of Oxidation Levels

Oxidation level is the percentage of the oxidized monomer units in the polymer film. For example, for oxidized polypyrrole, one out of three to four monomer units is oxidized. Since three to four monomer units share one positive charge, the oxidation level of polypyrrole is about 25%-33% [11]. Determination of oxidation level is a very important part of the study of conducting polymers. This work is usually done by chemically analyzing the compositions of the oxidized and reduced polymers [11-13]. Based on the same approach, the oxidation levels of poly(MeTh$_x$-MPMP$^+$) films were measured by x-ray emission analysis.

The oxidation levels of a group of 0.4 μm thick copolymers (MeTh:MPMP$^+$ ~ 1:1) deposited on carbon electrodes were determined. Copolymers were reduced at -0.20 V, or oxidized at various potentials. For each oxidized copolymer, the potential was scanned from 0.0 V to the desired value at a scan rate of 20 mV/s and the copolymer was taken out of the solution immediately the desired potential was reached. From the atomic ratios of the reduced copolymer, (Cl/S)$_{Red}$, and the

oxidized copolymer, $(Cl/S)_{Ox}$, the oxidation level of the copolymer at potential E can be calculated. If N is assumed to be the oxidation level at potential E, Cl_{Ox} and Cl_{Red} are the number of moles of ClO_4^- in the oxidized and reduced copolymer respectively, and $S(= S_{Ox} = S_{Red})$ is the number of moles of MeTh units in the copolymer, the following equation is valid:

$$Cl_{Ox} = Cl_{Red} + N(Cl_{Red} + S) \qquad (3.1)$$

Therefore, the oxidation level can be calculated by the rearrangement of equation 3.1:

$$N = [(Cl/S)_{Ox} - (Cl/S)_{Red}]/[(Cl/S)_{Red} + 1] \qquad (3.2)$$

Plots of oxidation level versus potential and voltammetric charge versus potential are shown in Fig.3.2. The charge was estimated from the areas indicated in Fig.3.3. It can be seen that when the potential is smaller than 1.20 V, the oxidation level increases with the potential, and is approximately proportional to the charge passed. From the voltammetric charge, Q_{cv}, and the polymerization charge, Q_{pol}, and assuming one monomer requires 2.2 electrons during the electrochemical polymerization (see section 1.2.2), as well as assuming the polymerization efficiency is 100%, the oxidation
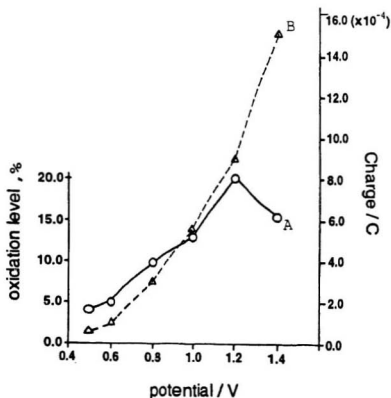
Fig.3.2. Oxidation level vs. potential (A), and voltammetric charge vs. potential (B) for copolymer films (0.4 μm, MeTh:MPMP⁺ ~ 1:1) generated from a 0.01 M MPMP⁺ + 0.2 M MeTh monomer solution containing 0.1 M Et₄NClO₄ /acetonitrile at a current density of 3.8 mA/cm².
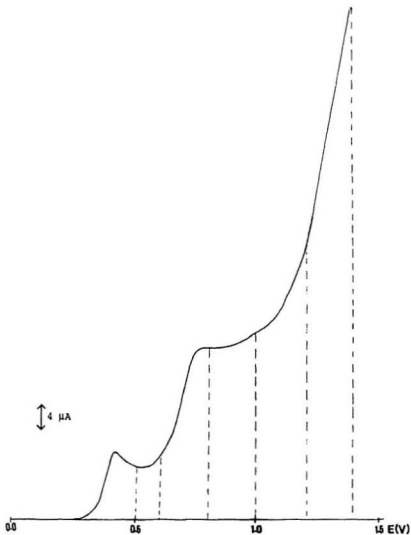
Fig.3.3. Charge estimated from cyclic voltammetry (scan rate = 20 mV/s) in acetonitrile containing 0.1 M Et$_4$NClO$_4$ for copolymers described in Fig.3.2.

level can also be estimated from cyclic voltammetry according to equation 3.3:

$$N = 2.2Q_{cv}/Q_{pol} \qquad (3.3)$$

A linear relationship was found between the oxidation level measured by x-ray emission analysis and that calculated from cyclic voltammetry when the potential was smaller than 1.2 V (Fig.3.4). At 1.4 V the copolymer was partly overoxidized so that the oxidation level was smaller than that at 1.2 V. The potential at which the oxidation level begins to decrease depends on factors such as the thickness of the copolymer film and how long the copolymer is held at each potential. For example, when the above copolymers were held at each potential for 5 minutes, the oxidation level began to decrease at less than 1.0 V. Since the copolymer has a very fast electrochemical response (see below), it is not necessary to hold the potential in order to achieve equilibrium if thin copolymer films are employed.

It was also observed that when oxidized copolymers were immersed in a stirred solvent at open circuit (water, acetone, acetonitrile, and methanol were tested), their oxidation levels decreased dramatically. This indicates that oxidized
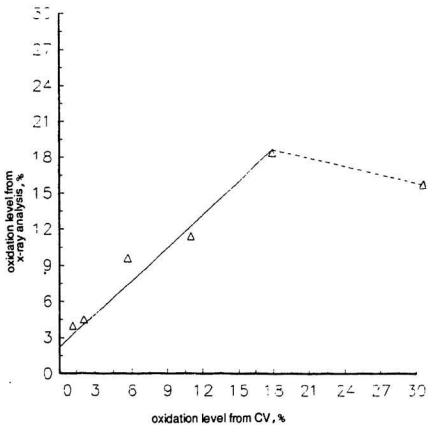
Fig.3.4. Oxidation level of poly(MeTh,-MPMP$^+$) from x-ray emission analysis vs. that from cyclic voltammetry.

copolymers are reduced or at least partly reduced by the solvent or an impurity.

The oxidation level of the as formed virgin poly-MeTh film was also estimated by x-ray emission analysis. The polymers were prepared on 0.0707 cm^2 carbon electrodes from acetonitrile containing 0.1 M MeTh + 0.1 M Et_4NClO_4 at current densities of 1.0 mA/cm^2 and 2.0 mA/cm^2 respectively for 96 seconds. The films were only washed with acetone before analysis. The average result of 28% ± 4% from 7 films is in good agreement with the values measured by elemental analysis [8].

3.2.4 Cyclic Voltammetry

Cyclic voltammograms of poly-MPMP$^+$, poly-MeTh and poly(MeTh$_n$-MPMP$^+$) are shown in Fig.3.5. The apparent formal potentials of poly-MPMP$^+$ and poly-MeTh are at about 0.70 V and 0.67 V, respectively. In contrast, the apparent formal potential of poly(MeTh$_n$-MPMP$^+$) is about 0.76 V, which is more positive than those of both poly-MPMP$^+$ and poly-MeTh. This may result from the overoxidation of the pyrrole rings during the copolymerization process. Moreover, the copolymer usually has a shoulder in the 0.40 V to 0.60 V region, the shape, height and exact position of which are influenced by
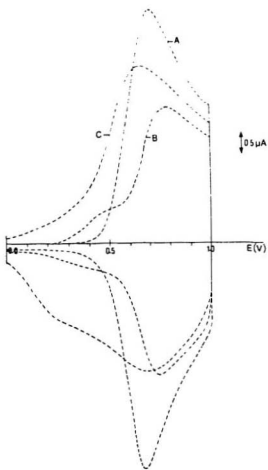
Fig.3.5. Cyclic voltammograms of A--poly-MPMP⁺ (0.3 μm [1]), B--poly(MeTh₄-MPMP⁺) (0.2 μm), and C--poly-MeTh (0.1 μm [10]) at a scan rate of 100 mV/s in acetonitrile containing 0.1 M Et₄NClO₄. The copolymer film (MeTh:MPMP⁺ ~ 1:1) was generated from a 0.002 M MPMP⁺ + 0.2 M MeTh monomer solution containing 0.1 M Et₄NClO₄/acetonitrile at a current density of 0.77 mA/cm².

the composition and the thickness of the film.

Poly(MeTh$_x$-MPMP$^+$) films generally exhibit a very fast electrochemical response. For a 0.2 μm thick copolymer film, there was a linear relationship between peak height and scan rate for scan rates up to 200 mV/s (Fig.3.6).

3.2.5 Film Morphology and Thickness

Scanning electron microscopy was used to study the morphology of copolymers deposited on indium/tin oxide-coated glass slides. Some results are shown in Fig.3.7. In one series of experiments, copolymers produced from different monomer solutions at the same current density were studied (pictures A and B). In another series of experiments, copolymers generated from 0.002 M MPMP$^+$ + 0.2 M MeTh at different current densities were compared (pictures C and D). By observing the surface of each copolymer film, it was concluded that the morphologies of copolymers are influenced by both the current density and the MeTh:MPMP$^+$ ratio in the monomer solution. For each monomer solution, the higher the current density, the less smooth the copolymer surface. At the same time, the higher the MeTh:MPMP$^+$ ratio in the monomer solution, the less smooth the copolymer surface produced under the same current density. From the broken cross section, all
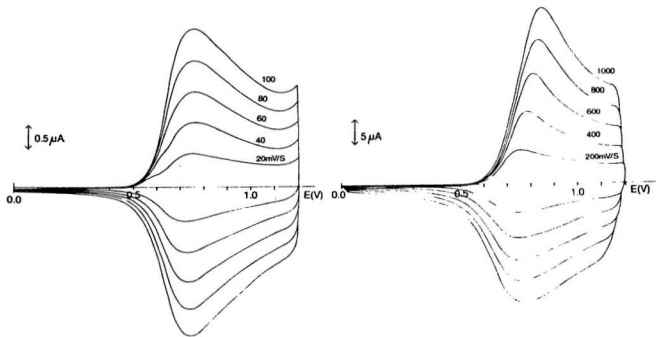
Fig 3.6. Cyclic voltammograms of a 0.2 μm thick copolymer film in acetonitrile containing 0.1 M Et$_4$NClO$_4$ at different scan rates. The copolymer was generated from a 0.01 M MPMP$^+$ + 0.2 M MeTh monomer solution containing 0.1 M Et$_4$NCl$_4$/acetonitrile at a current density of 0.77 mA/cm^2.

Fig.3.7. Influence of current density and monomer solution composition on morphology. Copolymers A and B were generated from 0.01 M MPMP$^+$ + 0.2 M MeTh and 0.5 mM MPMP$^+$ + 0.2 M MeTh monomer solutions respectively at a current density of 0.77 mA/cm^2. Copolymers C and D were produced from a 0.002 M MPMP$^+$ + 0.2 M MeTh monomer solution at current densities of 2.0 and 4.0 mA/cm^2 respectively. All the solutions contained 0.1 M Et$_4$NClO$_4$/acetonitrile.
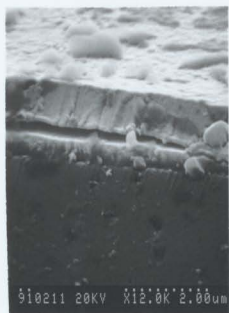
A
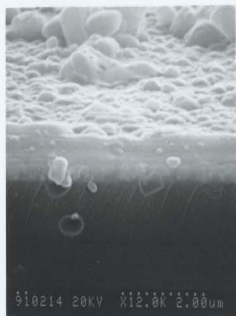
B
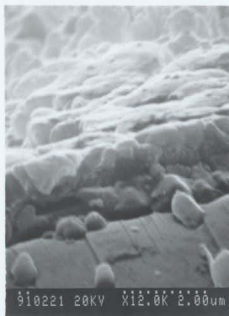
C
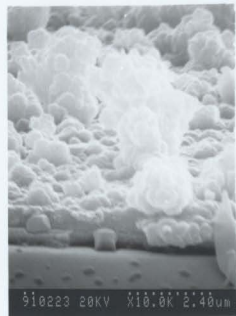
D

of the copolymer films seem to be very dense. It was also observed that the MeTh rich copolymers were easier to crack, while the MPMP$^+$ rich ones were easier to peel from the Pt electrode surface, especially when they were thick.

The influence of thickness on morphology was observed during the measurement of film thickness (see below). The result was that the thinner films were much smoother than the thicker ones of the same composition (Fig.3.8).

Scanning electron microscopy was also used to measure the thickness of copolymers deposited on the cylindrical surface of 0.127 mm diameter Pt wire. The diameter difference between a polymer-coated electrode and the bare Pt electrode is twice the film thickness (Fig.3.8).

If a copolymer has too rough a surface such as that in Fig.3.7-D, it is meaningless to measure its thickness. The current density and the composition of the monomer solution must therefore be carefully selected. The thicknesses of copolymer films with three different compositions were measured. The data show a linear relationship between charge density and film thickness (Fig.3.9). The average result is that a charge density of (0.20 ± 0.04) C/cm^2 is needed to

Fig.3.8. Determination of film thickness and influence of thickness on morphology. Copolymers B and C were of the same composition but different thickness (5.0 μm and 0.7 μm). They were produced from a 0.005 M MPMP$^+$ + 0.2 M MeTh monomer solution containing 0.1 M Et$_4$NClO$_4$/acetonitrile at a current density of 2.0 mA/cm^2 on 0.127 mm diameter Pt wire. Picture A was the bare Pt electrode.
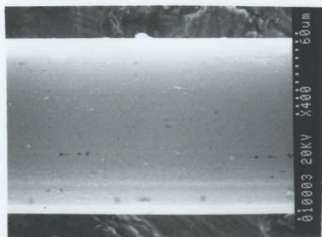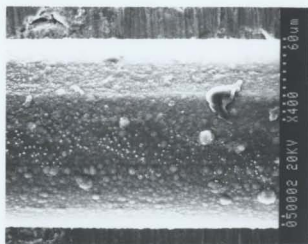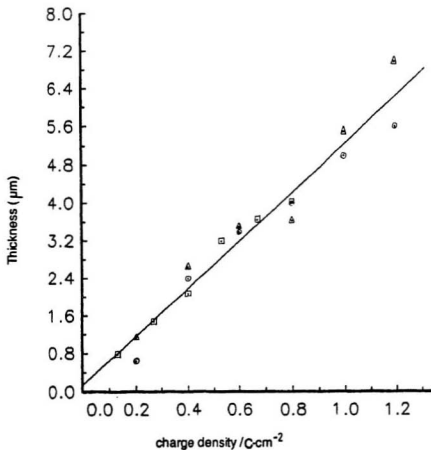
Fig.3.9. Thickness vs.charge density: ○--films (MeTh:MPMP⁺ ~ 0.52:1) were generated from a 0.005 M MPMP⁺ + 0.2 M MeTh monomer solution at a current density of 2.0 mA/cm²; ▲--films (MeTh:MPMP⁺ ~ 0.33:1) were generated from a 0.01 M MPMP⁺ + 0.2 M MeTh monomer solution at a current density of 1.0 mA/cm²; □--films (MeTh:MPMP⁺ ~ 0.30:1) were generated from a 0.01 M MPMP⁺ + 0.2 M MeTh monomer solution at a current density of 0.67 mA/cm². All the monomer solutions contained 0.1 M Et₄NClO₄/acetonitrile.

72
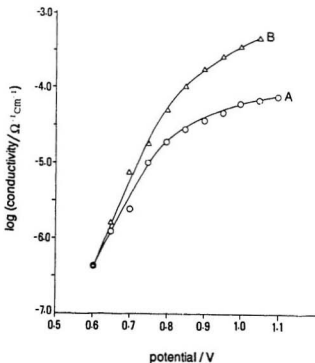
Fig.3.10. Log$_{10}$(electronic conductivity) vs. potential plots from dual electrode measurements. Curves A and B represent respectively the results for copolymers with MeTh:MPMP$^+$ ratios of 0.22:1 and 1:1. The copolymer films were generated from 0.01 M MPMP$^+$ + 0.1 M MeTh and 0.002 M MPMP$^+$ + 0.2 M MeTh monomer solutions respectively containing 0.1 M Et$_4$NClO$_4$/acetonitrile at a current density of 0.77 mA/cm^2. Each data point is an average for a 0.4 μm and a 0.8 μm film.

produce a 1.0-μm thick copolymer film. This result is between the charge densities needed to produce a 1.0 μm thick poly-MPMP+ film [13] and poly-MeTh film [10].

Because MeTh is smaller than MPMP+ in size, it was suggested that copolymers with a high MeTh content would be thinner than those containing less MeTh produced using the same charge density. However, since the experimental error exceeded any thickness difference resulting from different compositions, it was not reasonable to determine separately the charge density vs. thickness relationships for different composition copolymers. By comparison of the areas of cyclic voltammograms, it was found that the copolymerization efficiency did not change significantly with either the composition of the monomer solution or the polymerization current density. Therefore, in this work, a charge density of 0.20 C/cm^2 is assumed to produce a 1.0 μm thick copolymer film regardless of its composition and preparation conditions.

3.2.6 Electronic and Ionic Conductivities
3.2.6.1 Dual Electrode Method

The electronic conductivity vs. potential relationship can be easily determined by the dual electrode method (see section 2.6.1). Fig.3.10 shows the measured electronic

conductivities of two different composition copolymers as a
function of potential. To a good approximation, the
conductivities rise exponentially in the potential range of
0.60 V to 0.75 V. At higher potentials, the conductivities
rise at slower rates and appear to tend towards limiting
values. From a comparison of curves A and B, it can be
concluded that when the potential is higher than 0.60 V, the
higher MeTh content copolymer is more conductive.

No matter how fast the measurement is carried out, the
copolymer begins to overoxidize partly at about 0.9 V. The
true conductivities at higher potentials are presumably higher
than the results shown in Fig.3.10.

3.2.6.2 AC Impedance Method

AC impedance measurements can yield both the electronic
and ionic conductivity of a conducting polymer (see section
2.6.2). Copolymers prepared from different monomer solutions
were studied by this method. Since the results for different
compositions show similar correlations, only those for
copolymers from a 0.01 M MPMP$^+$ + 0.2 M MeTh monomer solution
are shown in Fig.3.11. The polymerization current densities
were selected according to the curves in Fig.3.1 so that the
percentage of MeTh in the copolymers was linearly related to
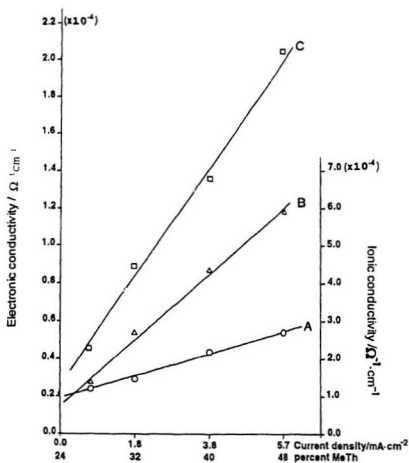
Fig.3.11. Conductivities vs. composition (and polymerization current density) from AC impedance measurements in acetonitrile containing 0.1 M Et₄NClO₄: A--ionic conductivity at 0.07 V; B--ionic conductivity at 0.92 V; C--electronic conductivity at 0.92 V. The copolymers (2.5 μm) were generated from a 0.01 M MPMP⁺ + 0.1 M MeTh monomer solution containing 0.1 M Et₄NClO₄/acetonitrile.

the current density. It can be seen that both the electronic and ionic conductivities increase with current density, or in other words, with the percentage of MeTh in the films. Moreover, the copolymers have different ionic conductivities in the reduced (at 0.07 V) and oxidized (at 0.92 V) forms, with the difference becoming greater for copolymers with higher MeTh contents.

3.3 DISCUSSION

It was observed that the monitored potential increased with the polymerization current density in the linear composition vs. current density regions shown in Fig.3.1. However, when the current density exceeded a certain value, the monitored voltage increased very little and sometimes did not increase at all. Connecting this observation with the composition results shown in Fig.3.1 may lead one to conclude that it is the potential, not the current density that determines the composition of a copolymer. When the potential is high enough to oxidize MeTh, the concentration of MeTh radical cation will increase rapidly with increasing the potential. On the other hand, the concentration of $MPMP^+$ radical cation can not be increased further at th electrode surface because it is diffusion controlled at this potential.

Therefore, the copolymer contains more MeTh as the potential is increased.

The linear relationship (slope ~ 0.9) between the oxidation levels measured by x-ray emission analysis and cyclic voltammetry when the potential is smaller than 1.2 V (Fig.3.4) reveals that it is valid to estimate oxidation levels from cyclic voltammetry. The plot does not pass through the origin. This may result from the larger errors when lower oxidation levels were estimated by both x-ray emission analysis and cyclic voltammetry.

The morphology of the copolymers provides some valuable information about the polymerization process. It is very clear from Fig.3.7-D that the copolymers grow in all three dimensions and not just in one or two. Also, it is easier to accept that large clumps of the copolymer seen in Fig.3.7-D were formed in the solution and then deposited onto the electrode surface than to accept that they were formed directly on the electrode surface.

Since the thinner polymer films are much smoother than the thicker ones prepared in this work, this may imply that a greater charge density per unit thickness is needed to produce

a copolymer film at the beginning of copolymerization, i.e. in the thinner film region. If this is true, estimation of the thickness of a thin polymer from the results for thick films may result in a significant error.

Comparing the electronic conductivities of copolymers at 0.92 V measured by the dual electrode method with those by AC impedance, it is found that the results are only in fair agreement. For example, the electronic conductivity of copolymers generated from a 0.002 M $MPMP^+$ + 0.2 M MeTh monomer solution at a current density of 0.77 mA/cm^2 (MeTh:$MPMP^+$ ~ 1:1), was estimated to be 0.8 x 10^{-4} $\Omega^{-1}cm^{-1}$ from AC impedance measurements, and 1.7 x 10^{-4} $\Omega^{-1}cm^{-1}$ from dual electrode measurements. The discrepancy may arise from two sources. The first one may be the density difference. The thinner copolymers in dual electrode measurements may be denser than the thicker ones in AC impedance measurements so that the former have higher electronic conductivity intrinsically even though they have the same composition. The second source of the discrepancy may be the error in estimating the thickness of thinner copolymer films as discussed previously.

The copolymers have not only higher electronic conductivities, but also higher ionic conductivities than

poly-MPMP$^+$. For example, at about 0.9 V, the electronic and ionic conductivities of poly-MPMP$^+$ are around 3 X 10^{-5} Ω^{-1}cm^{-1} and 5 X 10^{-5} Ω^{-1}cm^{-1} [4]; whereas, the electronic and ionic conductivities of poly(MeTh$_{1.0}$-MPMP$^+$) are about 2 X 10^{-4} Ω^{-1}cm^{-1} and 6 X 10^{-4} Ω^{-1}cm^{-1} respectively (Fig.3.11).

Both the electronic and ionic conductivities of the copolymers increase with increasing MeTh content. The increase in electronic conductivity results from the higher electronic conductivity of poly-MeTh compared with poly-MPMP$^+$. The increase in ionic conductivity may be because the higher MeTh content copolymer films are more porous (see section 3.2.5).

It can be seen from Fig.3.11 that the ionic conductivity of the reduced copolymer is smaller than that of the oxidized one, and the difference becomes larger as the MeTh content increases. This result reveals that the ionic conductivity is proportional to the concentration of the counter ion in a polymer film. Because the oxidized form has about 20% more counter ion, its ionic conductivity is higher than that of the reduced form. Since the counter ion concentration difference between the reduced and oxidized forms becomes larger for higher MeTh content copolymers, the ionic conductivity

difference is bigger for a higher MeTh content copolymer.

3.4 CONCLUSIONS

MeTh$_x$-MPMP$^+$ copolymers have been synthesized electrochemically from a wide compositional range of monomer solutions. Their compositions and oxidation levels were determined by x-ray emission analysis. A linear relationship between current density and the composition of the copolymer has been observed. Conductivity measurements indicated that both electronic and ionic conductivities of the copolymers are higher than those of poly-MPMP$^+$ and their values increase with increasing MeTh content.

REFERENCES

1. H. Mao and P.G. Pickup, *J. Phys. Chem.* **93**, 6480 (1989).

2. H. Mao, *Synthesis and Investigation of New Electronically and Ionically Conducting Polymers*, Ph.D. thesis (MUN, 1991).

3. H. Mao and P.G. Pickup, *J. Am. Chem. Soc.* **112**, 1776 (1990).

4. P.G. Pickup, *J. Chem. Soc., Faraday. Trans.* **86**, 3631 (1990).

5. G. Tourillon and F. Garnier, *J. Electroanal. Chem.* **135**, 173 (1982).

6. K. Kaneto, K. Yoshino, and Y. Inuishi, *Jpn. J. Appl. Phys.* **21**, L567 (1982).

7. E.K. Sichel, M. Knowles, M. Rubner, and J. Georges, *J.Phys.Rev.* **B25**, 5574 (1982).

8. G. Tourillon, in *Handbook of Conducting Polymers*, vol. 1, T.A. Skotheim, Ed. (Marcel Dekker, New York, 1986), pp. 293-350.

9. J. Roncali, *Chem. Rev.* **92**, 711 (1992).

10. J. Roncali, R. Garreau, A. Yassar, P. Marque, F. Garnier, and M. Lemaire, *J. Phys. Chem.* **91**, 6706 (1991).

11. M. Salmon, A.F. Diaz, A.J. Logan, M. Krounbi, and J. Bargon, *Mol. Cryst. Liq. Cryst.* **83**, 1297 (1983).

12. A. Dall'Olio, Y. Dascola, V. Varacca, and V. Bocchi, *Comptes Rendus Mathematiques de l'Academic des Sciences* **C267**, 433 (1968).

13. H. Mao and P.G. Pickup, *J. Electroanal. Chem.* **265**, 127 (1989).

Chapter 4 ELECTROSTATIC BINDING AND TRANSPORT OF

$$Fe(CN)_6^{3-/4-}$$

4.1 INTRODUCTION

The ability to preconcentrate electroactive species makes
an ionic conducting polymer-coated electrode very useful in
microanalysis and catalysis. Since $Fe(CN)_6^{3-/4-}$ possesses simple
electrochemistry, and its voltammetric peaks are usually far
away from those of the polymer itself, $Fe(CN)_6^{3-/4-}$ is commonly
used as the probe when positively charged polymers are
studied. Similar to poly-MPMP$^+$ [1-3], poly(MeTh$_x$-MPMP$^+$) has
been found to be able to bind $Fe(CN)_6^{3-/4-}$ electrostatically.
Therefore this copolymer has potential use in microanalysis
and catalysis. However, since an interesting variation of
voltammetric peak ratio with scan rate was observed, efforts
were concentrated on seeking the reasons for this unusual
phenomenon. When poly(MeTh$_x$-MPMP$^+$) films were studied in
aqueous K_2HPO_4 containing $K_3Fe(CN)_6$ (or $K_4Fe(CN)_6$), it was found
that the anodic to cathodic peak height ratio was about 1:1 at
high scan rates, but decreased to 0.75:1 at low scan rates.
All copolymer films (MeTh:MPMP$^+$ ~ 0.20:1) discussed in this
chapter were about 0.1 μm thick and were generated from a 0.01

M MPMP$^+$ + 0.2 M MeTh monomer solution containing 0.1 M
Et$_4$NClO$_4$/acetonitrile at a current density of 0.77 mA/cm^2,
unless otherwise stated.

4.2 RESULTS AND DISCUSSION

4.2.1 Cyclic Voltammetry

4.2.1.1 Saturation Process

Fig.4.1 shows cyclic voltammograms of MeTh-MPMP$^+$
copolymers at fast (100 mV/s) and slow (10 mV/s) scan rates in
aqueous 0.1 mM K$_3$Fe(CN)$_6$ + 0.1 M K$_2$HPO$_4$. When the copolymer is
immersed in the Fe(CN)$_6^{3-}$ solution, ClO$_4^-$ initially present in
the film as the counter ion, is replaced gradually by Fe(CN)$_6^{3-}$.
The voltammetric peaks due to Fe(CN)$_6^{3/4-}$ therefore increase
gradually. When all of the ClO$_4^-$ has been replaced, the
polymer is saturated with Fe(CN)$_6^{3/4-}$, and the voltammetric
peaks no longer increase. This is apparently true for the
saturation processes at both fast and slow scan rates.
However, it is interesting that the anodic to cathodic peak
height ratio is about 1:1 at a scan rate of 100 mV/s (Fig.4.1-
A), whereas the ratio is about 0.75:1 at 10 mV/s (Fig.4.1-B).

The detailed dependence of the anodic to cathodic peak
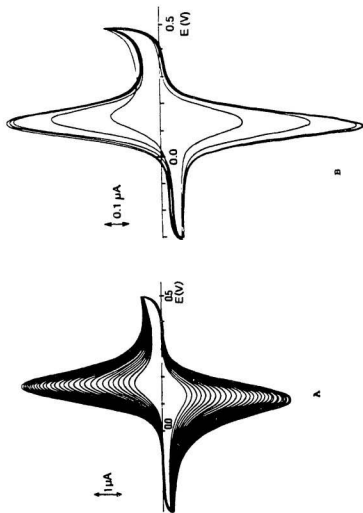
Fig. 4.1. Cyclic voltammograms during saturation of poly(MeTh, $-$MPMP$^+$) (0.1 μm) coated electrodes in aqueous 0.1 mM K$_3$Fe(CN)$_6$ + 0.1 M K$_2$HPO$_4$ at scan rates of 100 mV/s (A) and 10 mV/s (B).

height ratio on the scan rate is shown in Fig.4.2. It is clear that the ratio changes continuously from 1:1 at high scan rates to 0.75:1 at low scan rates. It should be mentioned that the anodic to cathodic peak height ratio is also dependent on the film thickness. It has been observed that a scan rate at which a thicker copolymer has nearly equal height oxidation and reduction peaks, can make a thinner copolymer show "0.75:1" peaks.

The ratio of 3/4:1 and the charge difference between $Fe(CN)_6^{3-}$ and $Fe(CN)_6^{4-}$ suggested that this phenomenon might arise from the accumulation of $Fe(CN)_6^{3-}$ in the film at slow scan rates. Based on this hypothesis, the following experiments were performed.

4.2.1.2 Influence of Holding Potential

4.2.1.2.1 In Aqueous $K_3Fe(CN)_6/K_2HPO_4$

In aqueous 0.1 mM $K_3Fe(CN)_6$ + 0.1 M K_2HPO_4, a copolymer saturated with $Fe(CN)_6^{3-/4-}$ at 100 mV/s as shown in Fig.4.1-A was first set at a potential of +0.5 V for 3 minutes. Then its potential was cycled between 0.5 V and −0.3 V at 100 mV/s. The cyclic voltammograms are shown in Fig.4.3. Interestingly, the first cathodic peak is approximately 30% higher than the following ones even at such a high scan rate. Several cycles
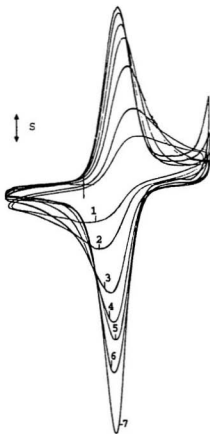
Fig.4.2. Cyclic voltammograms of a $Fe(CN)_6^{3-/4-}$ saturated poly(MeTh$_5$-MPMP$^+$) film (0.1 μm) in aqueous 0.1 mM $K_3Fe(CN)_6$ + 0.1 M K_2HPO_4 at different scan rates: 1--1000 mV/s, 2--500 mV/s, 3--200 mV/s, 4--100 mv/s, 5--50 mV/s, 6--20 mV/s, and 7--10 mV/s. The current scales were s = 10, 5, 2, 1, 0.5, 0.2, and 0.1 μA for scan rates of 1000, 500, 200, 100, 50, 20, and 10 mV/s, respectively.

were required before the cathodic peak reached a constant height (Fig.4.3-A), unless the potential was held at -0.3 V for a while during the first cycle (Fig.4.3-B).

4.2.1.2.2 In Aqueous K.HPO₄

A copolymer saturated with $Fe(CN)_6^{3-}$ at a constant potential of 0.5 V in aqueous 0.1 mM $K_3Fe(CN)_6$ + 0.1 M K_2HPO_4 was washed with H_2O and then transferred to aqueous 0.1 M K_2HPO_4 containing no $Fe(CN)_6^{3-}$. The potential was initially held at either -0.3 V or 0.5 V for 3 minutes. Cyclic voltammograms subsequently recorded at 100 mV/s are shown in Fig.4.4. When the initial potential is -0.3 V, the cyclic voltammogram exhibits constant anodic and cathodic peaks of equal height (Fig.4.4-A). When the initial potential is 0.5 V, the cathodic peak height changes rapidly, and the initial one is about 30% higher than the following anodic and cathodic peaks (Fig.4.4-B and 4.4-C). Furthermore, several scans were required for the cathodic peak height to become constant (Fig.4.4-B), unless the potential was held at -0.3 V for a while (Fig.4.4-C).

4.2.2 Discussion

The above experiments lead to the conclusion that holding the potential at 0.5 V can make the copolymer bind ~25% more
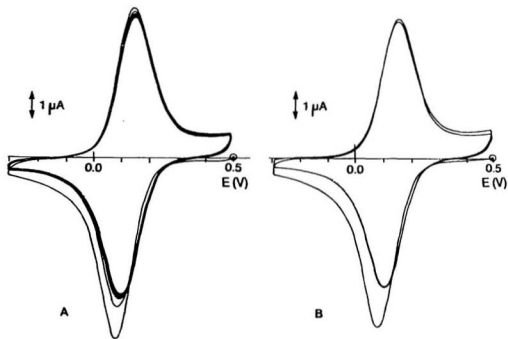
Fig.4.3. Influence of holding the potential at 0.5 V on cyclic voltammetry at a scan rate of 100 mV/s of a $Fe(CN)_6^{3/4}$ saturated poly(MeTh$_2$-MPMP$^+$) film (0.1 μm) in aqueous 0.1 mM $K_3Fe(CN)_6$ + 0.1 M K_2HPO_4: A--potential cycled continuously from 0.5 V; B--potential cycled from 0.5 V but interrupted at -0.3 V for 3 minutes during the first cycle.
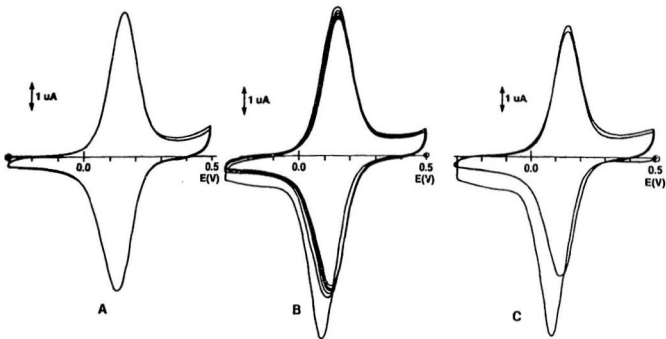
Fig. 4.4. Influence of holding the potential at −0.3 V or 0.5 V on cyclic voltammetry at a scan rate of 100 mV/s of a Fe(CN)$_6^{3/4}$ saturated poly(MeTh$_2$-MPMP$^+$) film (0.1 μm) in aqueous 0.1 M K$_2$HPO$_4$: A--potential cycled continuously from −0.3 V; B--potential cycled continuously from 0.5 V; and C--potential cycled from 0.5 V but interrupted at −0.3 V for 3 minutes during the first cycle.

$Fe(CN)_6^{3-/4-}$ than holding the potential at -0.3 V. This corresponds to the charge difference between $Fe(CN)_6^{3-}$ and $Fe(CN)_6^{4-}$. Also, the accumulated $Fe(CN)_6^{3-}$ will be released when the potential is cycled, and once the accumulated $Fe(CN)_6^{3-}$ has been released, it can not be accumulated again at a scan rate of 100 mV/s. This observation implies that if a polymer contains different amounts of $Fe(CN)_6^{3-}$ and $Fe(CN)_6^{4-}$, the anodic to cathodic peak height ratio will not be equal to one. Connecting this observation with the experimental results in Fig.4.1, it is realized that at 10 mV/s, ~25% more $Fe(CN)_6^{3-/4-}$ is taken up by the copolymer as $Fe(CN)_6^{4-}$ in the film is oxidized to $Fe(CN)_6^{3-}$. This excess $Fe(CN)_6^{3-/4-}$ is expelled when the $Fe(CN)_6^{3-}$ is reduced back to $Fe(CN)_6^{4-}$ (Eq.4.1).

$$\{Fe(CN)_6^{3-}\}_{pol} + e \underset{Ox.}{\overset{Red.}{\rightleftharpoons}} 3/4\{Fe(CN)_6^{4-}\}_{pol} + 1/4\{Fe(CN)_6^{4-}\}_{sol}$$

$$(4.1)$$
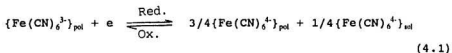
At fast scan rates, on the other hand, $Fe(CN)_6^{3-}$ can not be accumulated, which results in the copolymer containing the same amount of $Fe(CN)_6^{3-}$ and $Fe(CN)_6^{4-}$ at $+0.5$ V and -0.3 V, and their amounts do not change noticeably during the redox process. It must be other charged species that balance the excess charge during the redox process of $Fe(CN)_6^{3-/4-}$. The only

reasonable candidates are K^+ and HPO_4^{2-} (Eqs. 4.2 and 4.3). In order to clarify which one was involved, and to get some direct support for the above conclusion, x-ray emission analysis was performed.

$$\{K^+\}_{sol} + \{Fe(CN)_6^{3-}\}_{pol} + e \underset{Ox.}{\overset{Red.}{\rightleftharpoons}} \{Fe(CN)_6^{4-}\}_{pol} + \{K^+\}_{pol}$$

(4.2)

$$\{HPO_4^{2-}\}_{pol} + \{Fe(CN)_6^{3-}\}_{pol} + e \underset{Ox.}{\overset{Red.}{\rightleftharpoons}} \{Fe(CN)_6^{4-}\}_{pol} + \{HPO_4^{2-}\}_{sol}$$

(4.3)
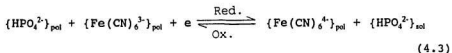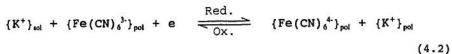
4.2.3 X-ray Emission Analysis

Eight 0.5 μm thick copolymer films deposited on 0.0707 cm^2 carbon electrodes were saturated with $Fe(CN)_6^{3-}$ at 0.5 V by immersing them in stirred aqueous 0.01 M $K_3Fe(CN)_6$ + 0.1 M K_2HPO_4 for 10 minutes. One of them was simply washed with water and then acetone before x-ray emission analysis. It was used as comparison standard (No. 1). For five of them, the potential was scanned slowly (10 mV/s) between 0.5 V and -0.3 V in aqueous 0.01 M $K_3Fe(CN)_6$ + 0.1 M K_2HPO_4 (No. 2 and 3), or 0.1 M K_2HPO_4 (No. 4, 5 and 6). Each film was held at each switching potential and the final potential for 5 minutes. For the other two films, the potential was rapidly scanned (100 mV/s) between 0.5 V and -0.3 V in aqueous 0.01 M $K_3Fe(CN)_6$

+ 0.1 M K_2HPO_4, and they were removed from the solution immediately the potential reached the final value. Each film was washed thoroughly with H_2O and then acetone before x-ray emission analysis. The results are shown in table 4.1. In the table, the atomic percentage of each element is defined as the atomic percentage of that particular element in the total of the following five detectable elements: S + Cl + P + K + Fe. The results were directly from the SQ software (see section 2.5) with no additional corrections, and therefore should be treated as semi-quantitative.

It can be seen that a significant amount of Fe is lost during the potential scan to -0.3 V (No. 2 and 4 vs. No. 1). When the potential is scanned back to 0.5 V, the initial $Fe(CN)_6^{3-}$ content is restored in 0.01 M $K_3Fe(CN)_6$ + 0.1 M K_2HPO_4 (No. 3), or HPO_4^{2-} is taken up in 0.1 M K_2HPO_4 (No. 5). Fig.4.5 compares the x-ray emission spectra of a virgin "as formed" copolymer, No. 3 copolymer, and No. 5 copolymer.

The detection of HPO_4^{2-} in copolymer 8 indicates that HPO_4^{2-} is the mobile ion at high scan rate. Since the Fe contents of copolymers 7 and 8 are similar to those of copolymers 1 and 3, and copolymer 8 contains less HPO_4^{2-} than copolymer 5, this may indicate that the electrochemistry of $Fe(CN)_6^{3-/4-}$ could not

Copolymer No.	1	2	3	4	5	6	7	8
Solution	0.01 M $K_3Fe(CN)_6$ +0.1 M K_2HPO_4			0.1 M K_3HPO_4			0.01 M $K_3Fe(CN)_6$ +0.1 M K_2HPO_4	
Potential program	.5V	.5V→ -.3V	.5V→ -.3V .5V	.5V→ -.3V	.5V→ -.3V→ .5V	.5V→ -.3V→ .5V -.3V	.5V→ -.3V	.5V→ -.3V .5V
Scan rate	Scanned at 10 mV/s then held at the final potential for 5 minutes						100 mV/s	
Atom% S[b]	63.6[c]	78.8	60.2	78.9	47.7	70.3	61.2	55.5
Atom% Cl	7.8[d]	6.4	2.9	8.2	-[e]	-	-	4.3
Atom% P	-	-	-	-	27.3	-	-	6.1
Atom% K	-	1.5	1.0	-	-	-	-	-
Atom% Fe	28.5	13.3	36.0	12.9	24.9	29.7	38.8	34.1

a--All copolymers (0.5 μm, MeTh:MPMP⁺ ~ 0.2:1) were generated at a current density of 0.77 mA/cm^2 from acetonitrile containing 0.01 M MPMP⁺ + 0.2 M MeTh + 0.1 M Et₄NClO₄.

b--Atomic percentage of each element was defined as the atomic percentage of that particular element in the total of the following five elements: S + Cl + P + K + Fe.

c--The results were directly from the "SQ" software (see section 2.5) without additional correction, and therefore should be treated as semiquantitative.

d--ClO₄⁻ was not completely replaced by $Fe(CN)_6^{3-}$ during the ion exchange process in aqueous 0.01 M $K_3Fe(CN)_6$ + 0.1 M K_2HPO_4.

e--Not detected.
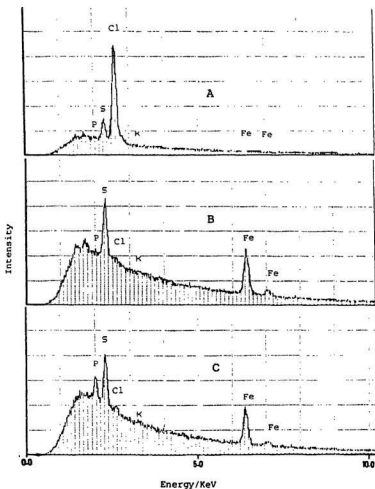
Fig. 4.5. Comparison of the x-ray emission spectra of (A) an as formed poly(MeTh$_{0.2}$-MPMP$^+$) film, (B) a Fe(CN)$_6^{3-}$ saturated poly(MeTh$_{0.2}$-MPMP$^+$) film whose potential was cycled from 0.5 V to -0.2 V then back to 0.5 V, and held at 0.5 V for 5 minutes in aqueous 0.01 M K$_3$Fe(CN)$_6$ + 0.1 M K$_2$HPO$_4$, and (C) a Fe(CN)$_6^{3-}$ saturated poly(MeTh$_{0.2}$-MPMP$^+$) film whose potential was cycled from 0.5 V to -0.2 V then back to 0.5 V, and held at 0.5 V for 5 minutes in aqueous 0.1 M K$_2$HPO$_4$.

follow the high scan rate so that quite large amounts of $Fe(CN)_6^{4-}$ remained when copolymers 7 and 8 were taken from the solution. The reason for the lag in the electrochemistry may be that (1) charge transfer between $Fe(CN)_6^{3-/4-}$ sites is not fast enough, (2) the migration of HPO_4^{2-} is not fast enough, or (3) the films were restructured to some degree (see chapter 5).

Table 4.1 also indicates that at equilibrium the copolymer does not contain HPO_4^{2-} in the presence of $Fe(CN)_6^{3-}$ in solution (No. 1, 2, and 3). This means that the ion exchange ability of HPO_4^{2-} is negligible compared with that of $Fe(CN)_6^{3-/4-}$ under these conditions. HPO_4^{2-} can only enter the copolymer when there is no alternative anion to balance the excess positive charge generated in the polymer electrochemically (No. 5), or during rapid electrochemical oxidation of $Fe(CN)_6^{4-}$ (No. 8).

It is somewhat surprising that K^+ is not involved in the redox process. K^+ should move more freely into and out of the copolymer, because it is smaller than HPO_4^{2-} and $Fe(CN)_6^{3-/4-}$, and has a smaller charge. In fact, when Na^+ was used instead of K^+ in these experiments, it did not enter the copolymer either (based on x-ray emission spectroscopy). Also, poly-MPMP$^+$ (see

section 2.3) behaved similarly to poly(MeTh$_x$-MPMP$^+$). Therefore, it seems that it is a general phenomenon that cations can not enter positively charged polymers such as poly(MeTh$_x$-MPMP$^+$) and poly-MPMP$^+$. This behaviour presumably arises from Donnan exclusion [4]. The electrostatic repulsion between the polymer's cationic sites and the cations in the solution prevents cations from entering the polymer film. On the other hand, anions are attracted by the polymer's cationic sites. Therefore, only anions can move into these positively charged polymers.

4.3 CONCLUSIONS

Since the excess positive charge produced by the oxidation of Fe(CN)$_6^{4-}$ is balanced by HPO$_4^{2-}$ at high scan rates, but by Fe(CN)$_6^{3-}$ at low scan rates, it can be concluded that HPO$_4^{2-}$ has a higher diffusion coefficient than Fe(CN)$_6^{3-/4-}$ in poly(MeTh$_x$-MPMP$^+$), but that Fe(CN)$_6^{3-/4-}$ is bound more strongly by the copolymer. In other words, HPO$_4^{2-}$ is kinetically favoured, while Fe(CN)$_6^{3-/4-}$ is thermodynamically favoured by the copolymer. At low scan rates, Fe(CN)$_6^{3-}$ has enough time to move into the copolymer and replace any HPO$_4^{2-}$ that may initially enter the copolymer. Therefore, the net process can be viewed as involving Fe(CN)$_6^{3-/4-}$ only. On the other hand, at high scan

rates, it is mainly HPO_4^{2-} that balances the excess charge accompanying each redox cycle. At intermediate scan rates, comparable amounts of HPO_4^{2-} and $Fe(CN)_6^{3-,4-}$ will be involved in the redox process.

REFERENCES

1. H. Mao, *Synthesis and Investigation of New Electronically and Ionically Conducting Polymers*, Ph.D. thesis (MUN, 1991).

2. H. Mao and P.G. Pickup, *J. Electroanal. Chem.* **265**, 127 (1989).

3. H. Mao and P.G. Pickup, *J. Phys. Chem.* **93**, 6480 (1989).

4. F.G. Donnan, *Chem. Rev.* **1**, 73 (1925).

Chapter 5 RESTRUCTURING OF CATIONIC POLYMERS BY Fe(CN)$_6$$^{4-}$

5.1 INTRODUCTION

When poly(MeTh$_4$-MPMP$^+$) was studied in aqueous K$_2$HPO$_4$ containing K$_3$Fe(CN)$_6$ (see chapter 4), it was found that after saturation the electrochemical response of Fe(CN)$_6$$^{3-/4-}$ within the copolymer began to decrease. After several hours, the voltammetric peaks nearly disappeared. This puzzling phenomenon is investigated in this chapter. All of the copolymer films discussed in this chapter were generated from a 0.01 M MPMP$^+$ + 0.2 M MeTh monomer solution containing 0.1 M Et$_4$NClO$_4$/acetonitrile at a current density of 0.77 mA/cm^2, unless otherwise stated.

5.2 RESULTS

5.2.1 Cyclic Voltammetry

Figure 5.1 shows the electrochemical response in the Fe(CN)$_6$$^{3-/4-}$ region of a poly(MeTh$_4$-MPMP$^+$) film in aqueous 0.1 mM K$_3$Fe(CN)$_6$ + 0.1 M K$_2$HPO$_4$. Fig.5.1-A shows the saturation process, during which Fe(CN)$_6$$^{3-}$ replaces ClO$_4$$^-$ that is initially present in the copolymer as the counter ion. Once all of the
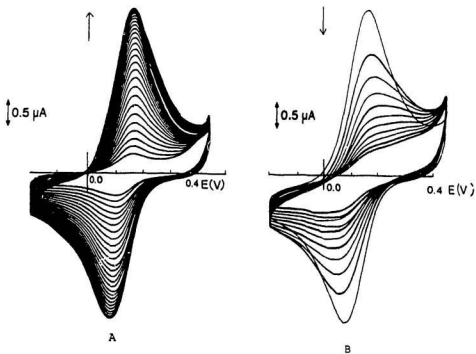
Fig.5.1. Cyclic voltammograms (100 mV/s) of a poly(MeTh$_4$-MPMP$^+$) film coated Pt electrode in 0.1 mM K$_3$Fe(CN)$_6$ + 0.1 M K$_2$HPO$_4$ (aq.) during continuous cycling at a scan rate of 100 mV/s: A—saturation process (peak currents increasing); B—decrease of peak height with time after saturation (cyclic voltammograms were recorded at 20 minutes intervals during which the potential was continuously cycled). The copolymer film (MeTh:MPMP$^+$ ~ 1:1, 0.15 μm) was produced at a current density of 0.77 mA/cm^2 from a 0.002 M MPMP$^+$ + 0.2 M MeTh monomer solution containing 0.1 M Et$_4$NClO$_4$/ acetonitrile.

ClO$_4^-$ had been replaced, the copolymer was saturated with Fe(CN)$_6^{3-/4-}$ as indicated by the constant voltammetric peak heights. Shortly after saturation (after about 5 cycles), the Fe(CN)$_6^{3-/4-}$ redox peaks began to decrease continuously (Fig.5.1-B). This was somewhat surprising because the copolymer was still in the solution containing Fe(CN)$_6^{3-}$. After about three hours, the Fe(CN)$_6^{3-/4-}$ peaks nearly disappeared as shown in Fig.5.1-B.

5.2.2 X-ray Emission Analysis

In order to determine whether the copolymer still contained Fe(CN)$_6^{3-/4-}$ after disappearance of the voltammetric peaks, x-ray emission analysis was performed. A group of 0.4 μm thick copolymers were generated on carbon electrodes. Half of them were just saturated with Fe(CN)$_6^{3-/4-}$ in 0.01 M K$_3$Fe(CN)$_6$ + 0.1 M K$_2$HPO$_4$ (aq.) with potential cycling, and then held at -0.2 V for 3 minutes. The remaining were left in the solution with continuous potential cycling for a longer time, until the Fe(CN)$_6^{3-/4-}$ voltammetric peaks became very small, and then held at -0.2 V for 3 minutes. The two groups of copolymers were thoroughly washed with water followed by acetone, and then analyzed by x-ray emission spectroscopy. The Fe emission peak from the Fe(CN)$^{4-}$ was compared with the S emission peak from the MeTh unit of the copolymer, which can be used as an

internal standard since all copolymers had the same composition. Even though x-ray emission analysis does not give the absolute amount of $Fe(CN)_6^{4-}$ in each copolymer, any difference in the content is reflected by the Fe to S peak area ratio. The results showed that the two groups of copolymers contained similar amounts of $Fe(CN)_6^{4-}$ (Fig.5.2). Therefore, the $Fe(CN)_6^{4-}$ content of the copolymers does not change significantly during the decrease of the $Fe(CN)_6^{3-/4-}$ electrochemical response. For convenience, the decreasing electrochemical response of the $Fe(CN)_6^{3-/4-}$ is called deactivation hereafter.

X-ray emission analysis was also used to investigate the deactivation process for a $Fe(CN)_6^{3-/4-}$ saturated copolymer in 0.1 M K_2HPO_4 (aq.) containing no $Fe(CN)_6^{3-}$. When a copolymer that was just saturated by $Fe(CN)_6^{3-/4-}$ was immersed in aqueous 0.1 M K_2HPO_4, the redox response of the $Fe(CN)_6^{3-/4-}$ also decreased gradually. It would be supposed that the decrease resulted from the replacement of $Fe(CN)_6^{3-/4-}$ by HPO_4^{2-} (or PO_4^{3-}, $H_2PO_4^-$). Surprisingly, x-ray emission analysis showed that there was no phosphorus in the copolymer at all, and the $Fe(CN)_6^{4-}$ content was similar to that before deactivation. Therefore, the deactivation presumably occurs by the same mechanism as in aqueous 0.1 M K_2HPO_4 containing $Fe(CN)_6^{3-}$.
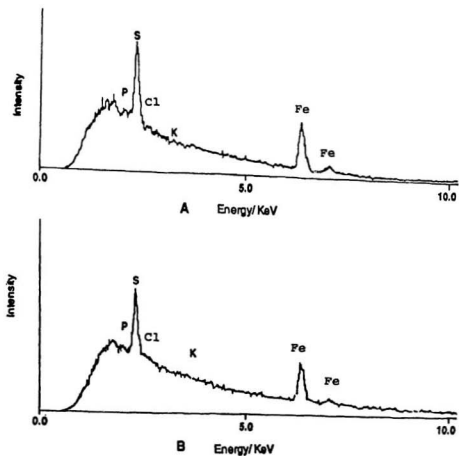
Fig.5.2. X-ray emission spectra of: A--a copolymer just saturated with Fe(CN)$_6^{4-}$ at -0.2 V in 0.01 M K$_3$Fe(CN)$_6$ + 0.1 M K$_2$HPO$_4$ (aq.); and B--a copolymer deactivated by Fe(CN)$_6^{4-}$ at -0.2 V in the same solution. The copolymers (MeTh:MPMP$^+$ ~ 0.37:1, 0.4 μm) were generated on carbon electrodes.

Since this result was rather unusual, I⁻ was tested instead of $Fe(CN)_6^{3-}$. After a copolymer was saturated with I⁻ in 0.01 M KI + 0.1 M K_2HPO_4 (aq.) at -0.2 V, the x-ray emission analysis was performed to get the relative amounts of I, P, S, Cl, and K in the copolymer. The copolymer was then immersed in stirred aqueous 0.1 M K_2HPO_4 containing no I⁻ for about 20 minutes at -0.2 V, after which another analysis was performed. The x-ray emission spectra are shown in Fig.5.3. It is clear that the copolymer contains only I⁻ following immersion in aqueous 0.01 M KI + 0.1 M K_2HPO_4 (Fig.5.3-A). This is similar to the result for $Fe(CN)_6^{3-}$. However, in contrast to the result for $Fe(CN)_6^{3-}$, I⁻ can be replaced by HPO_4^{2-}, although surprisingly, a considerable amount of I⁻ remains in the copolymer (Fig.5.3-B).

5.2.3 Decrease in the Diffusion Coefficient of $Fe(CN)_6^{3-/4-}$

Since the concentration of $Fe(CN)_6^{3-/4-}$ within the film is unchanged, it is deduced that the decrease of the voltammetric peak height must be due to slow charge transport in the film (see section 1.8.2). Charge transport can be treated as a diffusion process. Deactivation was therefore followed quantitatively by determining the charge transport diffusion coefficient as a function of time by chronoamperometry (see section 2.7.1). Since poly-MPMP⁺ has been found to behave
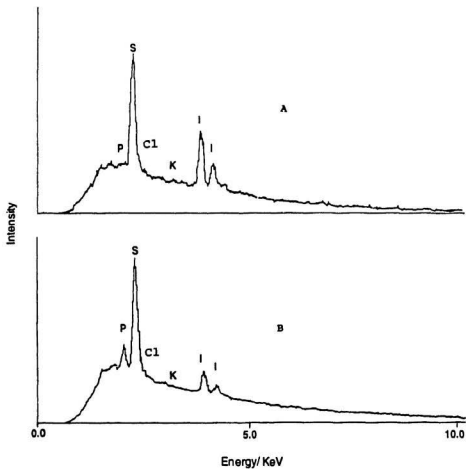
Fig.5.3. X-ray emission spectra of: A--a copolymer saturated with I⁻ in 0.01 M KI + 0.1 M K₂HPO₄ (aq.); and B--the above I⁻ saturated copolymer after immersion in stirred 0.1 M K₂HPO₄ (aq.) for 20 minutes at -0.2 V.

similarly to poly(MeTh$_n$-MPMP$^+$), the change of the charge transport diffusion coefficient of Fe(CN)$_6^{3-/4-}$ in poly-MPMP$^+$, along with the corresponding cyclic voltammograms, is shown in Fig.5.4 as an example. The charge transport diffusion coefficient and the cyclic voltammogram were measured or recorded at 25 minute intervals of potential cycling. It is clear that the decrease of the voltammetric peak height and the charge transport diffusion coefficient follow a similar trend. Therefore, the decrease of the electrochemical response of Fe(CN)$_6^{3-/4-}$ is caused by the decrease of the charge transport diffusion coefficient of Fe(CN)$_6^{3-/4-}$ within the polymer film.

5.2.4 Influence of Potential on Deactivation Speeds

Considering the charge difference between Fe(CN)$_6^{3-}$ and Fe(CN)$_6^{4-}$, it was expected that Fe(CN)$_6^{4-}$ and Fe(CN)$_6^{4-}$ might have different deactivation speeds in poly-MPMP$^+$. Fe(CN)$_6^{3-/4-}$ is in the Fe(CN)$_6^{3-}$ and Fe(CN)$_6^{4-}$ states at +0.5 V and -0.2 V, respectively. The change of charge transport diffusion coefficient of Fe(CN)$_6^{3-/4-}$ in poly-MPMP$^+$ is shown in Fig.5.5. The polymers were saturated with Fe(CN)$_6^{3-/4-}$ in 1 mM K$_3$Fe(CN)$_6$ + 0.1 M KNO$_3$ (aq.), and chronoamperometry was carried out in aqueous 0.1 M K$_2$HPO$_4$. Interestingly, deactivation mainly occurs at -0.2 V. In other words, only Fe(CN)$_6^{4-}$ deactivates
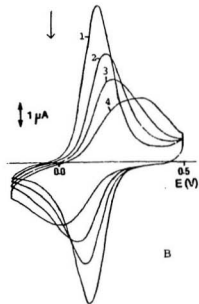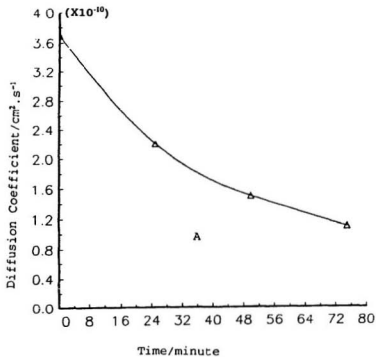
Fig.5.4. Comparison of the decreases in the charge transport diffusion coefficient (A) and the cyclic voltammetry (B) of $Fe(CN)_6^{3-/4-}$ within poly-MPMP$^+$ (0.2 μm) (see section 2.3). The potential was stepped from 0.4 V to -0.2 V when measuring the diffusion coefficients. Poly-MPMP$^+$ films were saturated with $Fe(CN)_6^{3-/4-}$ in 0.01 M $K_3Fe(CN)_6$ + 0.1 M K_2HPO_4(aq.). Scan rate = 100 mV/s.
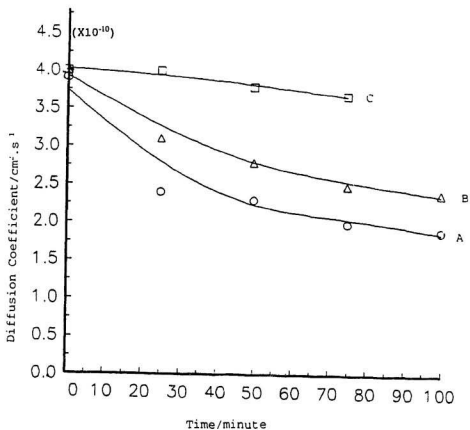
Fig.5.5. Charge transport diffusion coefficients for Fe(CN)$_6^{3-/4-}$ electrochemistry in poly-MPMP$^+$ (0.2 μm) as a function of time in 0.1 M K$_2$HPO$_4$ (aq.): A--potential held at -0.2 V between measurements; B--potential cycled between -0.2 V and 0.4 V at a scan rate of 10 mV/s; and C--potential held at 0.4 V between measurements. The potential was stepped from 0.4 V to -0.2 V when measuring the diffusion coefficients. Poly-MPMP$^+$ films were saturated with Fe(CN)$_6^{3-/4-}$ in 1 mM K$_3$Fe(CN)$_6$ + 0.1 M KNO$_3$ (aq.).

the polymer significantly; $Fe(CN)_6^{3-}$ does not.

5.2.5 Reactivation

In order to find out whether deactivation can be reversed, restructured copolymer films were examined in $NaClO_4$ (aq.). It is thought that if all the $Fe(CN)_6^{4-}$ can be replaced by ClO_4^-, the restructured film may be reactivated. $Fe(CN)_6^{3-/4-}$ was not taken up by the virgin poly(MeTh$_4$-MPMP$^+$) films in 1.0 mM $K_3Fe(CN)_6$ + 0.1 M $NaClO_4$ (aq.) as observed from the negative redox response of $Fe(CN)_6^{3-/4-}$. This would mean that 1.0 mM $Fe(CN)_6^{3-}$ could not compete with 0.1 M ClO_4^-. However, when a $Fe(CN)_6^{4-}$ restructured copolymer was immersed even in stirred 1.0 M $NaClO_4$ (aq.) at open circuit for one hour, and then transferred to 0.1 mM $K_3Fe(CN)_6$ + 0.1 M K_2HPO_4 (aq.), the copolymer showed a much smaller $Fe(CN)_6^{3-/4-}$ redox response, and the saturation speed was much slower when compared with virgin copolymers (Fig.5.6). This experiment has shown that restructured copolymer films can not be completely reactivated via ion exchange.

5.3 DISCUSSION

Since the amount of $Fe(CN)_6^{4-}$ does not change during the deactivation process, deactivation must result from a

110
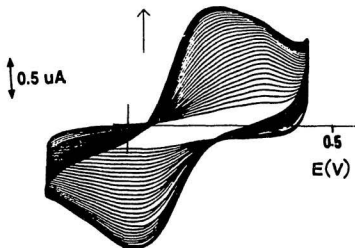
Fig.5.6. Cyclic voltammograms at a scan rate of 100 mV/s in 0.1 mM $K_3Fe(CN)_6$ + 0.1 M K_2HPO_4 (aq.) of a deactivated poly(MeTh$_4$-MPMP$^+$)$_4$(Fe(CN)$_6^{4-}$) film after treatment with 1.0 M NaClO$_4$ (aq.) for 1 hour. The copolymer's composition and thickness were the same as those in Fig.5.1.

structural change in the copolymer. In other words, $Fe(CN)_6^{4-}$ loses its electrochemical activity by changing the structure of the copolymer in a way that decreases its charge transport rate. The nature of this restructuring process is postulated below.

Each $Fe(CN)_6^{4-}$ ion entering the copolymer initially has no particular attraction to specific cationic sites. It will be loosely associated with a number of cationic sites as shown in Fig.5.7-A. As time passes, the $Fe(CN)_6^{4-}$ ion (or its derivatives formed under the electrochemical conditions studied [1-3]) and the cationic sites will adjust their relative positions and surroundings to maximize the strength of their association (Fig.5.7-B). This stronger association will gradually limit the mobility of the $Fe(CN)_6^{4-}$ ions. This isolation of $Fe(CN)_6^{4-}$ ions in turn leads to a slower charge transport rate between $Fe(CN)_6^{3-/4-}$ sites, regardless of whether charge is transferred by electron hopping between $Fe(CN)_6^{3-/4-}$ sites or by physical diffusion of $Fe(CN)_6^{4-}$ and $Fe(CN)_6^{3-}$ (see section 1.8.2). Therefore, a continuous decrease of the redox peaks shown in Fig.5.1-B results. Since $Fe(CN)_6^{4-}$ has higher charge than $Fe(CN)_6^{3-}$, the association is stronger, and so it can be immobilized more easily and rapidly. On the other hand, since $Fe(CN)_6^{3-}$ has a lower charge, it may not form
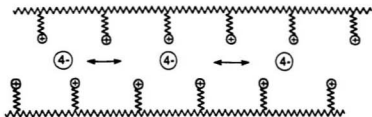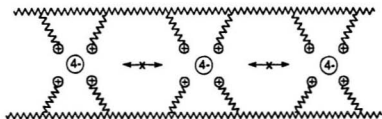
Fig.5.7. A postulated restructuring process: A--initially saturated copolymers, B--completely restructured copolymers.
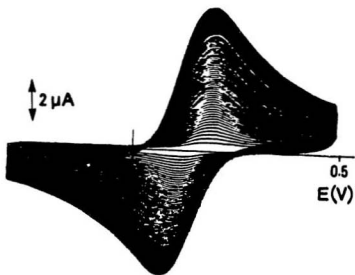
Fig.5.8. Cyclic voltammograms recorded during saturation of a 0.3 μm thick poly(MeTh$_x$-MPMP$^+$) film (MeTh:MPMP$^+$ - 0.37:1) in aqueous 0.1 mM K$_3$Fe(CN)$_6$ + 0.1 M K$_2$HPO$_4$ at a scan rate of 100 mV/s.

a sufficiently strong association with the cationic sites of the polymer for it to be effectively immobilized.

Restructuring may make thicker polymer films harder to saturate with $Fe(CN)_6^{4-}$ because the formation of a "net" like structure of the restructured polymer may prevent the entry of $Fe(CN)_6^{3-/4-}$ ions. During the saturation process, restructuring is presumably in progress near the polymer/solution interface where the polymer will already be saturated with $Fe(CN)_6^{4-}$. This will slow the movement of $Fe(CN)_6^{4-}$ ions toward the polymer/electrode interface, and hinder the entry of new $Fe(CN)_6^{4-}$ ions into the polymer. The slower movement of $Fe(CN)_6^{4-}$, at the same time gives $Fe(CN)_6^{4-}$ ions more time to restructure the polymer. These two effects enhance each other. The results are that the thicker polymer films are harder to saturate fully. As a result, the redox response of $Fe(CN)_6^{3-/4-}$ is smaller than it should be. Comparison of the redox responses of $Fe(CN)_6^{3-/4-}$ in copolymer films of different thickness demonstrates this. Fig.5.8 shows the saturation process for a 0.3 μm thick poly(MeTh$_x$-MPMP$^+$) film in aqueous 0.1 mM $K_3Fe(CN)_6$ + 0.1 M K_2HPO_4. It is clear that the saturation process is slow and that the electrochemical response of the $Fe(CN)_6^{3-/4-}$ saturated film is smaller than it should be compared with Fig.5.1-A. Therefore, in a study

where the peak height is important, the saturation process should be carried out as quickly as possible. Usually, thin polymer films and a high concentration of the electroactive species should be used. In the case of $Fe(CN)_6^{3-/4-}$, saturating the copolymer with $Fe(CN)_6^{3-}$ at an oxidizing potential where no significant restructuring occurs (eg. 0.4 V) can also achieve this goal.

Figure 5.5 shows that a polymer film can be restructured by $Fe(CN)_6^{4-}$ during potential cycling, but the restructuring rate is smaller than that at -0.2 V. Since $Fe(CN)_6^{4-}$ is continuously changed to $Fe(CN)_6^{3-}$ during potential cycling, the actual time allowed for $Fe(CN)_6^{4-}$ to restructure the polymer is much less than the time of the experiment, and a longer total time is needed. What is important here is that the copolymer can be restructured while the potential is cycled. This indicates that the association between $Fe(CN)_6^{4-}$ and the cationic sites is so strong, that once this association is formed, it can not be broken down electrochemically.

The fact that HPO_4^{2-} is not bound by the copolymer in the presence of $Fe(CN)_6^{3-/4-}$ or I^-, and HPO_4^{2-} is not able to displace any noticeable amount of $Fe(CN)_6^{3-/4-}$ from a copolymer even in 0.1 M K_2HPO_4 (aq.), indicates that HPO_4^{2-} is less favoured by the

copolymer. It is clear that the charge and size of HPO_4^{2-} are not the reasons, because they are between those of $Fe(CN)_6^{3-/4-}$ and I^-. A possible reason is that since HPO_4^{2-} is more strongly hydrated in solution, its partitioning into the film is disfavored.

REFERENCES

1. J. Kawiak, T. Jedral, and Z. Galus, *J. Electroanal. Chem.* **145**, 163 (1983).

2. S. Pons, M. Datta, J.F. McAleer, and A.S. Hinman, *J. Electroanal. Chem.* **160**, 369 (1984).

3. K. Niwa and K. Doblhofer, *Electrochimica Acta.* **31**, 439 (1986).

Chapter 6   REACTIVATION OF OVEROXIDIZED

POLY(3-METHYLTHIOPHENE)

6.1 INTRODUCTION

It is primarily the electronic conductivity that gives
conducting polymers their wide range of important applications
[1-10]. Since overoxidation causes conducting polymers to
lose their conductivities (see section 1.6), it limits their
applications, and is therefore a major concern. It would be
a significant development if overoxidation could be prevented,
or if the overoxidized polymers could be reactivated. Some
interesting work has been done in this area [11], but no
overoxidized polymers have been reactivated so far. After
some exploratory research, two novel methods for reactivating
poly(3-methylthiophene) overoxidized in solutions containing
Cl⁻ were discovered. Similar studies were carried out in Br⁻
and I⁻ solutions. The experimental details and our
explanations of the overoxidation and reactivation processes
will be presented in this chapter. Hopefully, this research
will provide some new ideas and thus inspire further studies
in this area.

Poly-MeTh films were prepared galvanostatically on 0.0052

119

cm^2 Pt electrodes and 0.0707 cm^2 carbon electrodes at a current density of 1.0 mA/cm^2 for 48 seconds and 96 seconds respectively from 0.1 M MeTh + 0.1 M Et$_4$NClO$_4$ in acetonitrile. The corresponding film thicknesses are about 0.1 μm and 0.2 μm [12]. The 0.1 μm thick polymer films were used in cyclic voltammetry experiments, and the 0.2 μm thick films were used for x-ray emission analysis, unless otherwise stated.

6.2 RESULTS

6.2.1 Overoxidation of Poly-MeTh in Acetonitrile Containing Cl$^-$

6.2.1.1 Cyclic Voltammetry

Poly-MeTh was rapidly overoxidized in acetonitrile containing 0.1 M Et$_4$NCl whenever the potential was greater than 0.8 V. Fig.6.1 shows the cyclic voltammograms during the overoxidation process, along with a cyclic voltammogram of a virgin poly-MeTh film in acetonitrile containing 0.1 M Et$_4$NClO$_4$. It is clear that the polymer is almost completely overoxidized in the Cl$^-$ solution during the first anodic scan, and that the charge under the first anodic scan is much higher than that for a virgin polymer in ClO$_4^-$ solution. When the overoxidation process was carried out in aqueous 0.1 M KCl or acetonitrile + 0.1 M Et$_4$PCl, similar results were obtained.
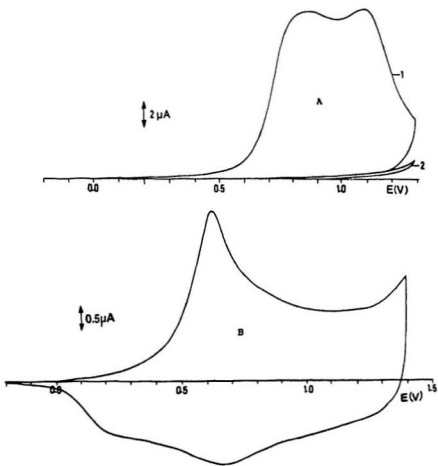
Fig.6.1. Cyclic voltammograms of poly-MeTh films (0.1 μm) in acetonitrile containing (A) 0.1 M Et₄NCl and (B) 0.1 M Et₄NClO₄. Scan rate ≈ 50 mV/s.

Moreover, poly(MeTh$_n$-MPMP$^+$) films (see chapter 3) behaved similarly to poly-MeTh in all the solutions mentioned above. Fig.6.2 shows the cyclic voltammograms of a poly(MeTh$_n$-MPMP$^-$) film in acetonitrile containing 0.1 M Et$_4$NClO$_4$ (curve 1) and 0.1 M Et$_4$NCl (curves 2 and 3). Curves 2 and 3 are the cyclic voltammograms during the first and second cycles in 0.1 M Et$_4$NCl solution.

6.2.1.2 X-ray Emission Analysis

In order to find out whether the overoxidized polymers contained chloride anion, Cl$^-$, x-ray emission analysis was performed. After polymers deposited on carbon electrodes were fully overoxidized in 0.1 M Et$_4$NCl/acetonitrile, they were immersed in stirred 0.1 M Bu$_4$NI/acetonitrile for 10 minutes. If the overoxidized polymer contains any Cl$^-$, it will be replaced by I$^-$. Then I will be detected by x-ray emission analysis, and the polymer will not show a Cl peak. Each film was thoroughly washed with acetone before x-ray emission analysis. The x-ray emission spectra, along with the Cl:S ratios, are shown in Fig.6.3.

The analysis showed that overoxidized polymers contained more Cl (Cl:S ~ 0.59:1) than an oxidized virgin polymer with ClO$_4^-$ as the dopant (Cl:S ~ 0.28:1), and no I was detected.
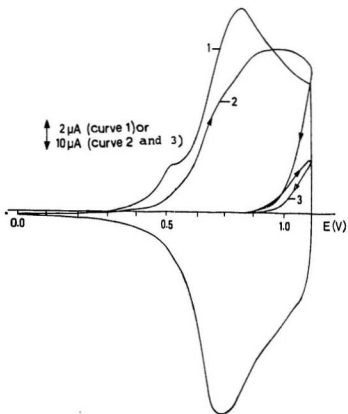
Fig.6.2. Cyclic voltammograms of poly(MeTh$_{1.0}$-MPMP$^+$) (see chapter 3) films (0.6 µm) in acetonitrile containing: 1--0.1 M Et$_4$NClO$_4$; and 2,3--0.1 M Et$_4$NCl (Curves 2 and 3 are the cyclic voltammograms during the first and second cycles, respectively). Scan rate = 100 mV/s.

Energy/ KeV

Energy/ KeV
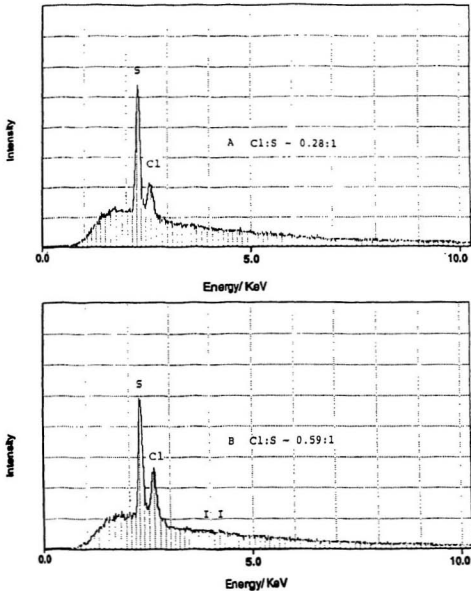
Fig. 6.3. X-ray emission spectra of: A--a virgin poly-MeTh film (0.2 μm) in the as formed state; and B--a poly-MeTh film (0.2 μm) overoxidized in 0.1 M Et_4NCl/acetonitrile by cycling the potential between -0.2 V and 1.4 V, and then immersed in a stirred Bu_4NI/acetonitrile for 10 minutes before x-ray emission analysis.

124

Also, for the overoxidized polymer films, holding the potential at 0.0 V or 1.3 V did not affect their chlorine content.

These experiments indicate that during overoxidation the polymer takes up more Cl, and Cl may become covalently bound to the polymer. From the Cl:S ratio of 0.59:1, it can also be concluded that every 1.5-2.0 monomer units of the overoxidized polymer possess one unexchangeable Cl atom.

6.2.2 Reactivation of Overoxidized Poly-MeTh Films

The loss of conductivity of a conducting polymer is usually caused by the loss of conjugation. The generally accepted overoxidation mechanism was discussed in section 1.6. Since Cl normally form a single bond in organic compounds, poly-MeTh overoxidized in Cl⁻ solution may contain the following unit:
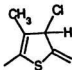
Therefore, if Cl or H can be eliminated, the conjugation can

be restored, and the polymer will be conductive again. Based on this hypothesis, we tried several methods, and two of them were found to work.

6.2.2.1 An Electrochemical Method

When the potential of an overoxidized poly-MeTh film was cycled in Et$_4$NClO$_4$/acetonitrile (the anion here was ClO$_4^-$ not Cl$^-$), no electrochemistry was observed at potentials below about 0.9 V (Fig.6.4). This means that the polymer was non-conductive. However, when the potential exceeded 0.9 V, a very steep and high anodic spike was observed at about 1.2 V. After this spike, the polymer showed cathodic and anodic peaks with a formal potential of about 1.08 V (Fig.6.4). Obviously, the polymer was conductive now indicating that it had been reactivated. It was also found that overoxidized poly-MeTh films can be reactivated by applying galvanostatically an anodic current (e.g. 0.5 mA/cm^2 for 10 seconds).

Since the formal potential of the reactivated polymer is much more positive than that of the virgin polymer, the two polymers must be different in some way. Since halogen substituted polythiophenes usually have higher formal potentials than polythiophene [13,14,15], it is reasonable to think that the difference may result from the elimination of

126
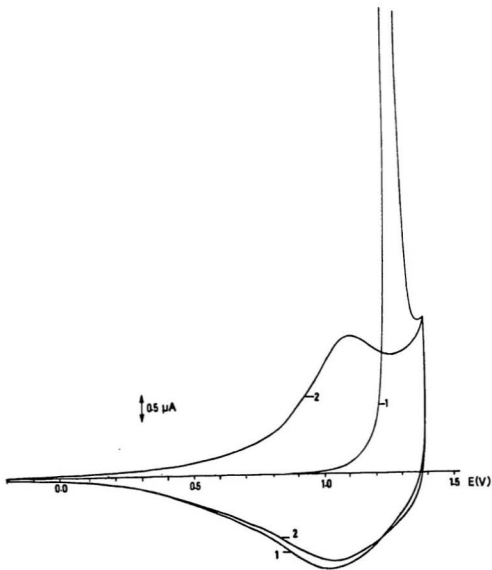
Fig.6.4. Cyclic voltammograms of an overoxidized poly-MeTh film (0.1 μm) during its electrochemical reactivation process in 0.1 M Et₄NClO₄/acetonitrile: 1--first scan; and 2--second scan. Scan rate = 50 mV/s.

H instead of Cl from the overoxidized poly-MeTh rings during
the reactivation process.

X-ray emission analysis showed that the oxidized form of
reactivated poly-MeTh films contained more Cl (Cl:S ~ 0.74:1)
than the overoxidized form (Cl:S ~ 0.59:1) (Fig.6.5). This
shows that the covalently bound chlorine is retained during
the reactivation process. The extra Cl intensity in the x-ray
emission spectrum of the reactivated poly-MeTh film simply
comes from ClO_4^- present in the polymer as the counter ion.

6.2.2.2 A Chemical Method

The electrochemical reactivation result indicates that H
is more easily eliminated than Cl. Since 2,3-dichloro-5,6-
dicyano-1,4-benzoquinone (DDQ) is a good dehydrogenation
reagent [16-18], and the dehydrogenation reaction can be
catalyzed by acids [18], DDQ was tested for the reactivation
of overoxidized poly-MeTh films in the presence of acid
catalysts.
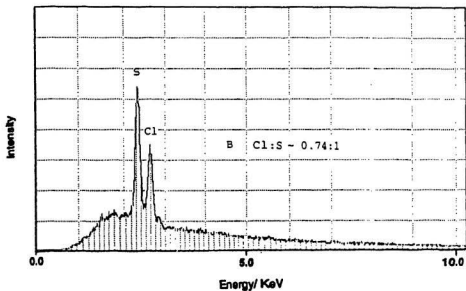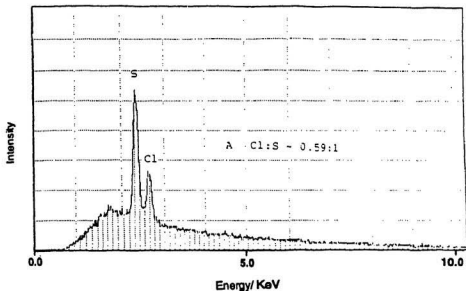
Fig.6.5. X-ray emission spectra of: A--a poly-MeTh film (0.2 μm) overoxidized in 0.1 M Et₄NCl/acetonitrile; and B--an oxidized poly-MeTh film (0.2 μm) overoxidized first and then reactivated in 0.1 M Et₄NClO₄/acetonitrile by cycling the potential.
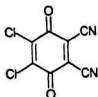
DDQ : 2,3 - Dichloro - 5,6 - dicyano - 1,4 - benzoquinone

Using a 0.05 M solution of DDQ in toluene containing 0.05 M HCl, overoxidized poly-MeTh films could be reactivated in 5 minutes under reflux conditions. The formal potential of the reactivated polymer was about 1.14 V in 0.1 M Et$_4$NClO$_4$/ acetonitrile (Fig.6.6). Since the polymer showed a redox response during the first anodic scan to 1.0 V, and it did not show a large sharp peak on the first scan to 1.3 V (cf. Fig.6.4), it is clear that it was a chemical reaction and not an electrochemical reaction that made the overoxidized polymer conductive again.

In 0.05 M DDQ + 0.05 M p-toluenesulphonic acid in toluene, overoxidized poly-MeTh films could also be reactivated in 5 minutes under reflux conditions. However, for films reactivated in this way, there were no clear anodic
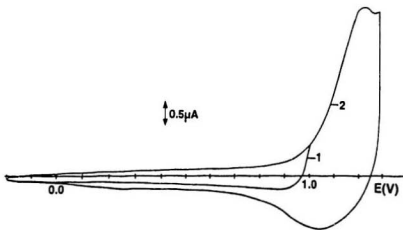
Fig.6.6. Cyclic voltammograms in 0.1 M Et₄NClO₄/acetonitrile after treatment of an overoxidized poly-MeTh film (0.1 μm) with 0.05 M DDQ + 0.05 M HCl in toluene under reflux for 5 minutes: 1--first scan, and 2--second scan. Scan rate = 50 mV/s.

and cathodic peaks between -0.2 V and 1.4 V (Fig.6.7).

6.2.2.3 Unsuccessful Methods

Since thermal heating is a method used commonly to form double bonds [19-23], a thermal method was tested. The overoxidized poly-MeTh film was heated to about 200 °C under vacuum. Electroactivity was checked by cyclic voltammetry several times as the temperature was increased. Once the temperature reached 200 °C, the polymer was kept at this temperature for three hours. During this time electroactivity was also checked several times. At no point in the experiment did the polymer show any sign of being reactivated. Therefore, thermal heating can not reactivate overoxidized poly-MeTh films, at least under the conditions studied.

Considering the oxidizing property of $Fe(CN)_6^{3-}$ [24], overoxidized poly-MeTh films were also treated with aqueous 0.1 M $K_3Fe(CN)_6$ both at room temperature and under reflux. The results showed that overoxidized poly-MeTh films could not be reactivated by this method either.
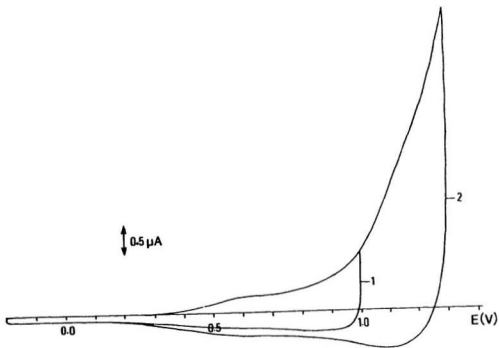
Fig.6.7. Cyclic voltammograms in 0.1 M Et₄NClO₄/acetonitrile after treatment of an overoxidized poly-MeTh film with 0.05 M DDQ + 0.05 M p-toluenesulphonic acid in toluene under reflux for 5 minutes: 1--first scan, and 2--second scan. Scan rate = 50 mV/s.

6.2.3 Overoxidation and Reactivation in Acetonitrile
Containing Bu₄NBr

6.2.3.1 Cyclic Voltammetry

Since Br^- is oxidized at about 0.6 V, and the oxidation peak was large, it was not possible to observe the polymer's redox peaks in 0.1 M Bu₄NBr/acetonitrile (Fig.6.8). Because the polymer coated electrode could still oxidize Br^- even after being held at 1.4 V for several minutes (Fig.6.8-B), it seems that the polymer remains conductive. This was surprising and unexpected. When the polymer was transferred to 0.1 M Et₄NClO₄/acetonitrile, it did show a redox response (Fig.6.9). These results indicate that the poly-MeTh film is not overoxidized in Bu₄NBr/acetonitrile under the conditions studied.

6.2.3.2 X-ray Emission Analysis

X-ray emission analysis showed that poly-MeTh films contained covalently bound Br after they had been electrochemically cycled in 0.1 M Bu₄NBr/acetonitrile even though they were not overoxidized. The x-ray emission spectra, along with Br:Cl:S ratios, are shown in Fig.6.10-A. The Br:S ratio for a poly-MeTh film was about 0.73:1 after the potential was cycled between -0.2 V and 1.4 V, and then held at 1.4 V for 3 minutes in 0.1 M Bu₄NBr/acetonitrile
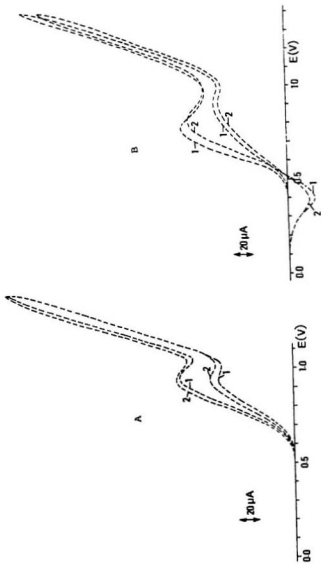
Fig.6.8. Cyclic voltammograms in 0.1 M Bu₄NBr/acetonitrile of: A—a bare Pt electrode; and B—a poly-MeTh film (0.1 µm) coated electrode. 1—first scan, and 2—second scan. Scan rate = 50 mV/s.
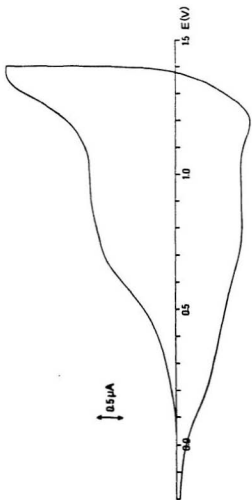
Fig.6.9. Cyclic voltammograms of a poly-MeTh film (0.1 µm) in Et$_4$NClO$_4$/acetonitrile after treatment in 0.1 M Bu$_4$NBr/acetonitrile by cycling the potential between -0.2 V and 1.4 V. Scan rate = 50 mV/s.
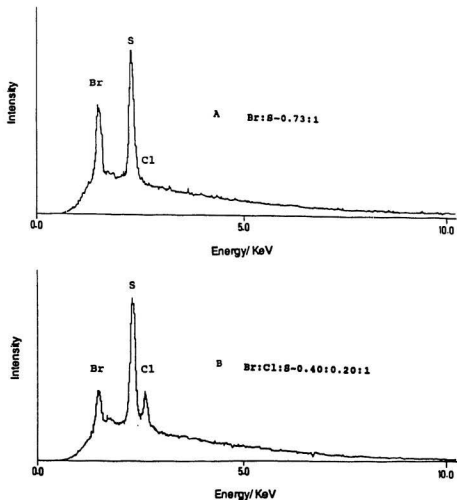
Fig.6.10. X-ray emission spectra of: A--a poly-MeTh film whose potential was cycled between -0.2 V and 1.4 V and then held at 1.4 V for 3 minutes in 0.1 M Bu₄NBr/acetonitrile; and B--a poly-MeTh film whose potential was held at 1.4 V for 3 minutes in 0.1 M Et₄NClO₄/acetonitrile after treatments as stated in A.

(Fig.6.10-A). When a poly-MeTh film was transferred to 0.1 M Et_4NClO_4/acetonitrile and held at a potential of 1.4 V after it had been cycled in 0.1 M Bu_4NBr/ acetonitrile, it did show a Cl peak, but the Br peak was still present with the Br:Cl:S ratio of 0.40:0.20:1 (Fig.6.10-B). Obviously, the Cl peak is caused by ClO_4^- present in the polymer as the counter ion, and the remaining Br is possibly covalently bound to the polymer. These experiments indicate that a poly-MeTh film contains two kinds of Br after its potential is cycled in 0.1 M Bu_4NBr/ acetonitrile and then held at 1.4 V. One kind is Br atoms covalently bound to the polymer. The other kind is bromide anion, Br^-, present as the counter ion. It is Br^- that is replaced by ClO_4^-.

6.2.4 Results in Acetonitrile Containing Bu_4NI

When the studies were repeated in 0.1 M Bu_4NI/ acetonitrile, the polymer could not be overoxidized even at a potential of 1.4 V. This was similar to the results for Br^- solution. However, x-ray emission analysis showed that the polymer contained no covalently bound I. This shows a difference from the reactions in Br^- solution.

6.3 DISCUSSION

Since a poly-MeTh film begins to overoxidize at around 0.8 V in 0.1 M Et₄NCl/acetonitrile, before Cl⁻ can be oxidized to Cl₂ (Fig.6.11), the overoxidation must result from a reaction involving Cl⁻. Figure 6.12 shows the postulated overoxidation mechanism in Cl⁻ solution. The first step is the oxidation of the monomer unit (I) to its charged species (II). Because it is still debatable whether polarons or bipolarons are the dominant charged species in oxidized poly-MeTh [15], II is only a simplification of the real form. After this initial oxidation, there is a nucleophilic addition reaction between Cl⁻ and II to form III. Since III is not conjugated, the polymer is no longer conductive.

This overoxidation mechanism is similar to those discussed in section 1.6. However, it is believed that a ketone is not formed, otherwise, the overoxidized polymers should not be reactivated by the two methods mentioned above. Our overoxidation process is also totally different from the "deactivation" process described by Harada and coworkers which was thought to be caused by the accumulation of bulky cations in the polymer film [11]. They refer to overoxidation as "degradation", and claim that the conductivity of a degraded
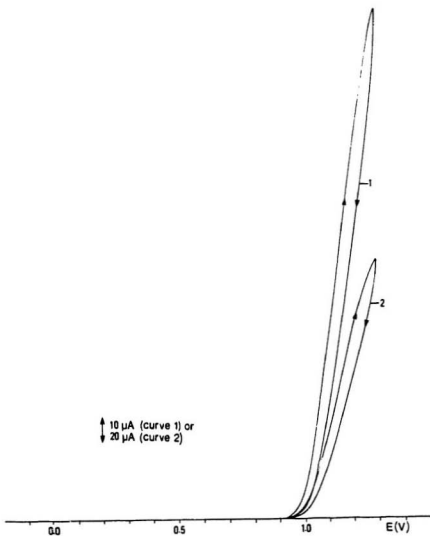
Fig.6.11. Cyclic voltammograms of the oxidation of Cl⁻ on a bare Pt electrode in acetonitrile containing 0.1 M Et₄NCl. Scan rate = 50 mV/s.
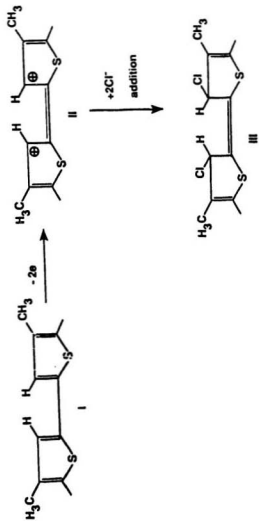
Fig.6.12. A postulated overoxidation mechanism for poly-MeTh in acetonitrile containing Cl.
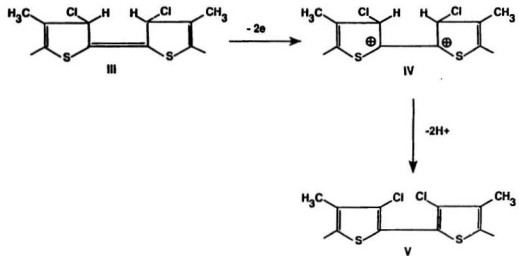
Fig.6.13. A proposed electrochemical reactivation mechanism for overoxidized poly-MeTh in acetonitrile containing ClO_4^-.

film can not be recovered. Our results have proven that this is wrong.

Figure 6.13 shows the proposed reactivation process. When III is taken up to a potential above 0.9 V in a non-nucleophilic electrolyte solution (e.g., Et$_4$NClO$_4$/ acetonitrile), it can be oxidized to form structures like IV. IV can easily convert to V by losing two protons. Since V is conjugated, the polymer becomes conductive again.

In the presence of Br$^-$, the reaction scheme is similar, but reactivation occurs simultaneously with overoxidation. A tentative mechanism is shown in Fig.6.14. The difference relative to Cl$^-$ is that III' can be further oxidized in Br$^-$ solution at the potential at which the nucleophilic addition of Br$^-$ occurs. Therefore, III' is converted to IV' once it is produced. Since IV' is conjugated, the polymer remains conductive.

It should be pointed out that all the structures in Fig.6.12 to Fig.6.14 are schematic simplifications of the real forms. For example, the positive charges on structure II may not be adjacent to each other, but delocalized along a certain length of the polymer chains.
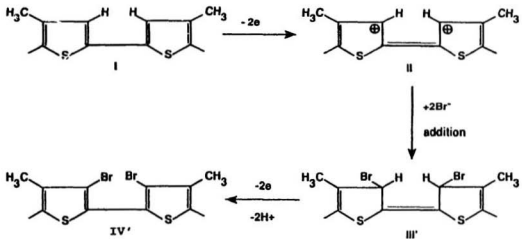
Fig.6.14. A tentative reaction mechanism for poly-MeTh in acetonitrile containing Bu₄NBr.

The difference between Cl⁻ and Br⁻ may result from the difference in electronegativity between Cl and Br. Since Cl has higher electronegativity, it can more effectively decrease the π-electron density along the polymer chains to make the polymer harder to oxidize. Thus, contrary to III' in Fig.6.14, III in Fig.6.12 can not be oxidized in Cl⁻ solution at the potential at which the nucleophilic addition of Cl⁻ occurs.

Since Br⁻ is oxidized to Br$_2$ in the reactions shown in Fig.6.14, there is no evidence to rule out the possibility that it may be Br or Br$_2$ and not Br⁻ that reacts with the charged species (II). Also, it is not understood why III can be reactivated in ClO$_4$⁻ solution, but not in Cl⁻ solution. The absence of a reaction between oxidized poly-MeTh and I⁻ may be due to the low nucleophilicity of I⁻, or the ease with which I⁻ is oxidized to I$_2$.

REFERENCES

1. L. Alcacer, Ed., *Conducting Polymers: Special Applications* (D.Reidel Publishing Company, Dordrecht(Holland), 1987).

2. D.B. Cotts and Z. Reyes, Eds., *Electrically Conductive Organic Polymers for Advanced Applications* (Noyes Data Corporation, New Jersey, 1986).

3. M. Gauthier, M. Armand, and D. Muller, in *Electroresponsive Molecular and Polymeric Systems*, vol. 1, T.A. Skotheim, Ed. (Marcel Dekker, New York and Basel, 1988), pp. 41-95.

4. H.D. Abruna, in *Electroresponsive Molecular and Polymeric Systems*, vol. 1, T.A. Skotheim, Ed. (Marcel Dekker, New York and Basel, 1988), pp. 97-171.

5. M.A. Marcus, in *Electroresponsive Molecular and Polymeric Systems*, vol. 1, T.A. Skotheim, Ed. (Marcel Dekker, New York and Basel, 1988), pp. 173-195.

6. A.G. MacDiarmid and M. Maxfield, in *Electrochemical Science and Technology of Polymers*, vol. 1, R.G. Linford, Ed. (Elsevier Applied Science, London and New York, 1987), pp. 67-101.

7. A.B. Hillman, in *Electrochemical Science and Technology of Polymers*, vol. 1, R.G. Linford, Ed. (Elsevier Applied Science, London and New York, 1987), pp. 241-291.

8. H. Munstedt, in *Electronic Properties of Polymers and Related Compounds*, H. Kuzmany, M. Mehring, and S. Roth, Eds. (Springer-Verlag, Berlin, 1985), pp. 8-17.

9. H. Kuzmany, M. Mehring, and S. Roth, Eds., *Electronic Properties of Conjugated Polymers III: Basic Models and Applications* (Springer-Verlag, Berlin, 1989).

10. T.A. Skotheim, Ed., *Handbook of Conducting Polymers*, vol. 1 (Marvel Dekker, New York and Basel, 1986).

11. H. Harada, T. Fuchigami, and T. Nonaka, *J. Electroanal. Chem.* **303**, 139 (1991).

12. J. Roneali, R. Garreau, A. Yassar, P. Marque, F. Garnier,

and M. Lemaire, *J. Phys. Chem.* **91**, 6706 (1991).

13. G. Tourillon, in *Handbook of Conducting Polymers*, vol. 1, T.A. Skotheim, Ed. (Marcel Dekker, New York and Basel, 1986), pp. 293-350.

14. G. Tourillon and F. Garnier, *J. Electroanal. Chem.* **161**, 51 (1984).

15. J. Roncali, *Chem. Rev.* **92**, 711 (1992).

16. D. Burn, D.N. Kirk, and V. Petrow, *Proc. Chem. Soc.*, 14 (1960).

17. H.J. Ringold and A.B. Turner, *Chem. and Ind.*, 211 (1962).

18. A.B. Turner and H.J. Ringold, *J. Chem. Soc. (C)*, 1720 (1967).

19. D.G. Ballard, A. Courtis, I.M. Shirley, and S.C. Taylor, *J. Chem. Soc., Chem. Commun.*, 954 (1983).

20. S. Yamada, S. Tokito, T. Tsutsui, and S. Saito, *J. Chem. Soc., Chem. Commun.*, 1448 (1987).

21. I. Murase, T. Ohnishi, T. Noguchi, and M. Hirooka, *Polym. Commun.* **25**, 327 (1984).

22. D.R. Gagnon, J.D. Capistran, F.E. Karasz, and R.W. Lenz, *Polym. Bull.* **12**, 293 (1984).

23. G. Kossmehl, M. Hartel, and G. Manecke, *Makromol. Chem.* **131**, 15 (1970).

24. P. Ribereau and P. Pastour, *Bull. Soc. Chim. Fr.*, 2076 (1969).